



NTNU – Trondheim
Norwegian University of
Science and Technology

Verification of simulation program for high head hydro power plant with air cussion

Even Lillefosse Haugen

Master of Energy and Environmental Engineering

Submission date: June 2013

Supervisor: Torbjørn Kristian Nielsen, EPT

Norwegian University of Science and Technology
Department of Energy and Process Engineering

EPT-M-2013-49

MASTEROPPGAVE

for

Stud.techn. Even Lillefosse Haugen

Våren 2013

Verifikasjon av simuleringsprogram for vannkraftverk med luftputekammer

Verification of simulation program for high head hydro power plant with air cushion.

Bakgrunn og målsetting

I prosjektoppgaven har kandidaten laget et program som simulerer trykksvingninger ved start og stopp av et høytrykks vannkraftanlegg, eksemplifisert ved Driva kraftverk ved Sunndalsøra. I dette kraftverket er det luftputekammer i stedet for konvensjonelt svingekammer. Luftputekammer er kritisk mhp nivåsvingninger pga faren for at luftputa skal unnslippe og ekspandere ut gjennom tilløpstunnelen.

For å verifisere simuleringsprogrammet skal det gjennomføres målinger av trykksvingningene i Driva kraftverk. Imidlertid bør simuleringsprogrammet forbedres på noen punkter.

Det er også av interesse å utvide programmet til å omfatte generatoren og tilknytning til nettet. Dermed kan verifisering av simuleringene skje ved en kontinuerlig måling av ledeapparat og nettfrekvens.

Oppgaven bearbeides ut fra følgende punkter

- 1 Implementering av en mer detaljert turbinmodell, enten ved bruk av endimensjonal turbinmodell på differensialligningsform eller ved bruk av såkalte Suther-kurver
- 2 Implementere generator i programmet
- 3 Planlegge målinger på kraftverket
- 4 I samarbeid med kraftverket, instrumenter og gjennomføre målinger

” - ”

Senest 14 dager etter utlevering av oppgaven skal kandidaten levere/sende instituttet en detaljert fremdrift- og eventuelt forsøksplan for oppgaven til evaluering og eventuelt diskusjon med faglig ansvarlig/veiledere. Detaljer ved eventuell utførelse av dataprogrammer skal avtales nærmere i samråd med faglig ansvarlig.

Besvarelsen redigeres mest mulig som en forskningsrapport med et sammendrag både på norsk og engelsk, konklusjon, litteraturliste, innholdsfortegnelse etc. Ved utarbeidelsen av teksten skal kandidaten legge vekt på å gjøre teksten oversiktlig og velskrevet. Med henblikk på lesning av besvarelsen er det viktig at de nødvendige henvisninger for korresponderende steder i tekst, tabeller og figurer anføres på begge steder. Ved bedømmelsen legges det stor vekt på at resultatene er grundig bearbeidet, at de oppstilles tabellarisk og/eller grafisk på en oversiktlig måte, og at de er diskutert utførlig.

Alle benyttede kilder, også muntlige opplysninger, skal oppgis på fullstendig måte. For tidsskrifter og bøker oppgis forfatter, tittel, årgang, sidetall og eventuelt figurnummer.

Det forutsettes at kandidaten tar initiativ til og holder nødvendig kontakt med faglærer og veileder(e). Kandidaten skal rette seg etter de reglementer og retningslinjer som gjelder ved alle (andre) fagmiljøer som kandidaten har kontakt med gjennom sin utførelse av oppgaven, samt etter eventuelle pålegg fra Institutt for energi- og prosesssteknikk.

Risikovurdering av kandidatens arbeid skal gjennomføres i henhold til instituttets prosedyrer. Risikovurderingen skal dokumenteres og inngå som del av besvarelsen. Hendelser relatert til kandidatens arbeid med uheldig innvirkning på helse, miljø eller sikkerhet, skal dokumenteres og inngå som en del av besvarelsen. Hvis dokumentasjonen på risikovurderingen utgjør veldig mange sider, leveres den fulle versjonen elektronisk til veileder og et utdrag inkluderes i besvarelsen.

I henhold til "Utfyllende regler til studieforskriften for teknologistudiet/sivilingeniørstudiet" ved NTNU § 20, forbeholder instituttet seg retten til å benytte alle resultater og data til undervisnings- og forskningsformål, samt til fremtidige publikasjoner.

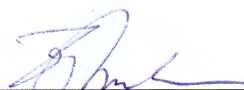
Besvarelsen leveres digitalt i DAIM. Et faglig sammendrag med oppgavens tittel, kandidatens navn, veileders navn, årstall, instituttnavn, og NTNUs logo og navn, leveres til instituttet som en separat pdf-fil. Etter avtale leveres besvarelse og evt. annet materiale til veileder i digitalt format.

- Arbeid i laboratorium (vannkraftlaboratoriet, strømningsteknisk, varmeteknisk)
 Feltarbeid

NTNU, Institutt for energi- og prosesssteknikk, 14. januar 2013



Olav Bolland
Instituttleder



Torbjørn K. Nielsen
Faglig ansvarlig/veileder

Preface

This thesis was written at the Waterpower Laboratory, Department of Energy and Process engineering at the Norwegian University of Science and Technology during the spring of 2013. The purpose of the thesis was to create a simulation algorithm with a simple GUI that ended up not being that simple.

Should anyone wish to implement and improve the model described in this thesis, it is my hope that the work presented herein will aid them in this endeavour.

I would like to thank my supervisor Professor Torbjørn Kristian Nielsen, who usually finds time to answer my ill-timed questions, despite always being busy, and doing so with good spirits. A special thanks also goes to Post-Doc Pål-Tore Storli and PhD student Bjørn Winther Solemslie for listening to (and answering) my questions, regardless of their relevance or intelligence. I would also like to thank senior analyst Gunnar Aronsen at Trønderenergi Kraft AS for supplying me with data and knowledge about the Driva system.

Writing this thesis has yielded much factual knowledge, but also experience in prioritizing. One cannot do everything, implement every idea or simulate every scenario.

Even Lillefosse Haugen
Trondheim, June 10, 2013

Abstract

Europe's energy production is experiencing a shift towards larger volumes of renewable energy. This development, however beneficiary, poses several challenges. One of them being the lack of regulation, as the energy is available when nature permits. As a consequence, Norwegian hydroelectric plants, risk operating under conditions not anticipated in their planning/construction stage. This occurs during large influx of unregulated power, where grid stability needs to be maintained by these plants. Presented herein is a model implemented to investigate grid influence on system components, down to the waterway. The model was verified on the Driva hydropower system. The background data was provided by Norconsult, as the measurements could not be conducted by the author himself. This was due to circumstances around the plant owners.

Simulated load rejections overestimated the runaway speed and slightly underestimated the pressure surge, compared to measured data. Simulated behaviour of remaining online unit seemed reasonable and maintained good stability. The model output compares well with analytical solutions. The turbine model behaved as expected during transient load changes, however unit output did not change as expected when changing the grid frequency. This was a result of the governor models not operating as expected. The model was also able to simulate highly undesirable conditions in the waterway due to grid frequency fluctuations.

The program generally compare well with rejection trial data as well as expected physical behaviour of the various components. A few points for improvement was suggested, including a further investigation into the governor models.

Sammendrag

Europas energiproduksjon opplever et skifte mot mer fornybar energi. Denne utviklingen er fordelaktig, men byr på flere utfordringer. En av disse er mangelen på regulering og kontroll, da denne energien er tilgjengelig når naturen tillater det. Som et resultat risikerer norske vannkraftverk å måtte takle forhold som ikke var forutsett under planlegging og konstruksjon av disse. Dette skjer når store mengder fornybar energi flyter inn i nettet, og nettstabilitet må holdes av disse verkene. For å undersøke hvordan forhold i nettet påvirker systemkomponenter, ble det implementert en model som kan simulere alle komponenter fra strømmnett til vannvei. Modellen ble deretter verifisert ved målinger fra Driva kraftverk. Bakgrunnsdata ble levert av Norconsult ettersom forfatteren ikke hadde anledning til å gjøre målinger selv. Dette var grunnet forhold hos eieren av kraftverket.

Simulerte lastavslag overestimerte rusningsturtallet og underestimerte resulterende trykkstøt noe, sammenlignet med målte verdier. Simulert oppførsel hos aggregatet som ikke gikk i avslag stemte overens med det som var forventet, og viste god stabilitet. Modellen viser god nøyaktighet sammenlignet med kjente analytiske uttrykk. Oppførsel hos turbinen under transient lastendring virket rimelig, men effekt ut av aggregatet endret seg mye mindre enn forventet. Dette var fordi regulatormodellene ikke opererte som forventet. Modellen klarte også å simulere uheldige forhold i vannveien som en følge av svingninger i nettfrekvensen.

Programmet gir stort sett sammenfallende resultater med avlagsmålinger samt forventet fysisk oppførsel av de forskjellige komponentene. Et par forbedringer ble foreslått, blant annet en nærmere undersøkelse av regulatormodellene.

Contents

Preface	iii
Abstract	v
Sammendrag	vii
Nomenclature	xiii
1 Introduction	1
1.1 Background	1
1.2 Previous work	2
2 Theory	3
2.1 Fluid conduits	3
2.1.1 Water hammer	4
2.1.2 Pressure propagation	5
2.1.3 Water conduit model	6
2.2 Surge control	8
2.2.1 Surge Chamber model	9
2.3 Turbine	11
2.3.1 Spiral casing and guide vanes	12
2.3.2 Runner	13
2.3.3 Self governing	14
2.3.4 Draft tube	14
2.3.5 Turbine Losses	15
2.3.6 Turbine model	16
2.4 Generator	18
2.4.1 Elementary concepts	18

2.4.2	Generator model	20
2.5	Power system and grid	22
2.5.1	Frequency and flywheel mass	22
2.5.2	Load distribution and permanent speed droop	23
2.5.3	Grid modelling	23
2.6	Governing	24
2.6.1	PID regulator	25
2.6.2	Governor modelling	27
2.7	Turbine/generator coupling	28
3	Model implementation	29
3.1	General description	29
3.2	Input/Output	33
3.3	Expandability	34
4	Model calibration and discussion	35
4.1	The Driva system	35
4.2	Tunnel frictional loss coefficients	37
4.3	Turbine time constants	38
4.4	Turbine frictional loss coefficients	39
4.5	Turbine hydraulic losses	39
5	Results and discussion	41
5.1	Load Rejection	42
5.1.1	Rejection unit two over 5.9s from 81.16 MW	42
5.1.2	Rejection unit one over 8.4s from 78.12 MW	46
5.2	Immediate closure of both units	50
5.3	Load variations	51
5.3.1	Step variation	51
5.3.2	0.6 % sine variation with period equal to oscillation period	55
6	Conclusion and further work	57
	List of Figures	59
	List of Tables	61
	Bibliography	64

A	Model source code	67
B	GUI Screenshot	85
C	Simulation parameters for performed simulations	87
D	Method of Characteristics	89
	D.1 Finite difference discretization	90
	D.2 Grid representation and computational aspects	91
	D.3 Boundary and initial conditions	92
E	Driva system data	93
F	Rejection Trials Driva	97

Nomenclature

δ	Magnetic reference angle	<i>rad</i>
δ_b	Permanent speed droop	—
δ_t	Transient speed droop	—
κ	Turbine opening degree	—
ω	frequency	<i>rad/s</i>
ρ	Water density	<i>kg/m³</i>
σ	Self governing parameter	—
C_m	C- characteristic constant	<i>m</i>
C_p	C+ characteristic constant	<i>m</i>
K_m	Magnetic constant	—
T_a	Acceleration time constant	<i>s</i>
T_c	Closure time of valve/turbine	<i>s</i>
T_r	Wave reflection time	<i>s</i>
V_{gas}	Gas volume	<i>m³</i>
A	Area	<i>m²</i>
a	Speed of sound	$\frac{m}{s}$

B	MOC constant	$\frac{s}{m^2}$
c	Servo acceleration	$\frac{m}{s^2}$
D	Tunnel diameter	m
dt	Time increment	s
dx	Length increment	m
E	Voltage	V
f	friction coefficient	m
g	acceleration of gravity	$\frac{m}{s^2}$
H	head	m
I	Current	A
J	Polar moment of inertia	$\frac{kg}{m^2}$
L	Length of tunnel	m
N	Number of tunnel sections	—
n	Polytropic exponent	—
n	Rotational speed	rpm
P	Power	W
Q	volume flow	$\frac{m^3}{s}$
R	Head loss factor per section of pipe	$\frac{s^2}{m^5}$
T	Torque	Nm
V	Velocity	$\frac{m}{s}$

Subscripts

0	Initial condition
1	Inlet condition
2	Outlet condition

A	Previous lengthwise position
B	Next lengthwise position
i	Grid position index
P	Current timestep value
R	Reference condition
t	Time derivative
x	Position derivative

Abbreviations

GUI	Graphical User Interface
MOC	Method of Characteristics
PID	Proportional Integral Derivative (Refers to a regulator)
RPM	Revolutions Per Minute

Chapter 1

Introduction

1.1 Background

A hydropower system consists of various components interlinked by fluid conduits. A change in load demand in the electric power grid, will necessitate a regulation of the turbine, as well as the attached generator. This will result in a change of flow velocity at one point in the system. This, in turn, results in a change in pressure that will propagate throughout the system via the conduits.

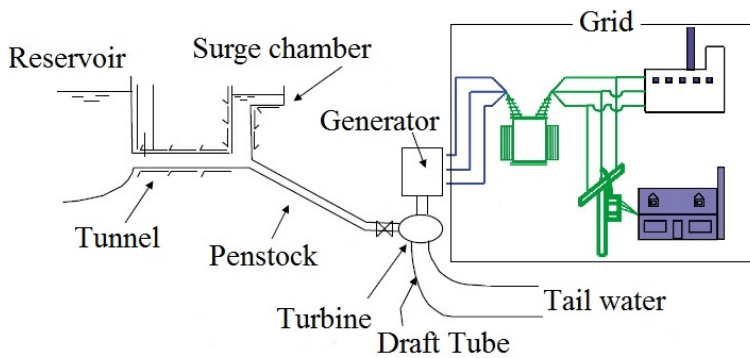


Figure 1.1: Principal sketch of a hydropower system[8]

These fluctuations will influence upstream components, and when the pressure wave reflects and returns, the behaviour of the turbine-generator assemblies themselves. These fluctuations are a disturbance in the system, originating from variations in the power grid. Europe's energy production is experiencing a shift towards larger volumes of renewable energy. This development, however beneficiary, poses several challenges. One of them being the lack of regulation, as the energy is available when nature permits. As a consequence, Norwegian hydroelectric plants, risk operational conditions not anticipated during their planning/construction. This occurs during large influx of unregulated power, where grid stability needs to be maintained by these plants. To investigate grid influence on system components, a simulation model that can model all components from grid to reservoir was implemented.

1.2 Previous work

The turbine model utilized in this thesis has been developed by professor, and director of the Hydropower Laboratory at NTNU, Torbjørn Nielsen as a part of his doctoral thesis[9]. He has also written several short papers about this model [10] [11]. He has also co-authored an introductory report along with Finn O. Rasmussen [11], relating to the use of this model. It is the hope of the author that he will, through this thesis, aid in its verification and further use.

Chapter 2

Theory

The purpose of this chapter is to provide the reader with a brief overview as to how hydropower systems operate, in order to supply users connected to the power grid with stable reliable power when demand dictates. An introduction to the properties of fluid conduits, hydropower system components and their interaction will be given. Methods of modelling individual components will also be suggested, and used in the subsequent chapter to construct a simulation algorithm.

2.1 Fluid conduits

In order to investigate the effects and consequences of regulatory events in a hydropower system, insight into how pressure will propagate through the system along with its magnitude is needed. The unsteady flow behaviour in a pipe system due to a regulatory disturbance is called surge. Surge occurs when the volumetric flow rate is changed, and due to the inertia of the masses of moving water. The positive pressure surge due to closing equipment, such as valves and turbines, is also referred to as water hammer.[15]

For a circular pipe, the continuity and momentum equations can be written as

$$gH_x + V_t + \frac{f}{2D}V|V| = 0 \quad (2.1)$$

$$H_t + \frac{a^2}{g} V_x = 0 \quad (2.2)$$

where

g	-	Gravitational acceleration
H_x	-	Head position derivative
H_t	-	Head time derivative
f	-	Darcy Friction factor
V	-	Velocity
a	-	Wave propagation speed (speed of sound)
D	-	Tunnel diameter

(2.1) accounts for the frictional loss of pressure due to contact between the flowing fluid and the wall. An approximation of the Darcy-Weisbach friction factor is used.

2.1.1 Water hammer

When the volumetric flow is reduced, a retardation of the water string is induced at the point of regulation. In order to counteract the momentum of this retardation, kinetic energy is transferred to pressure energy, causing pressure to increase. The magnitude of theoretical water hammer is given by Joukowsky as[8]

$$\Delta H = \frac{a\Delta Q}{gA} \quad (2.3)$$

A	-	Tunnel area
Q	-	Flow

(2.3) is valid for immediate closure, defined as closure time T_c faster than the wave reflection time given by (2.5). For closures over a time $T_c \gg T_r$

$$\Delta H = \frac{a\Delta Q}{gA} \frac{T_r}{T_c} \quad (2.4)$$

It becomes evident from (2.3) and (2.4) that the largest magnitude of water hammer occurs with a total retardation of the water. It is also dependant on tunnel cross-sectional area. A negative water hammer will occur for a acceleration of the water.

2.1.2 Pressure propagation

When the mass of moving water is large, such as in systems with long tunnels, water acts as a compressible, or elastic, fluid. Due to this elasticity, disturbances will propagate along the water conduit after occurring. The wave travels from the point of disturbance origin to the closest free water surface. The wave-front will travel with the wave propagation speed, also known as the speed of sound a . The value of a in water is not constant, but for flow in rigid pipes without air entrainment, it is approximately $1200 \frac{m}{s}$. Upon encountering a free water surface, the wave will reflect and travel back through the conduit, eventually reaching back to the location of origin, where another reflection will occur. Worst-case scenarios occur when positive pressure peaks propagating along a conduit amplify each other, becoming a source of major disturbance in the system. To avoid this, understanding of the surge reflection time is essential

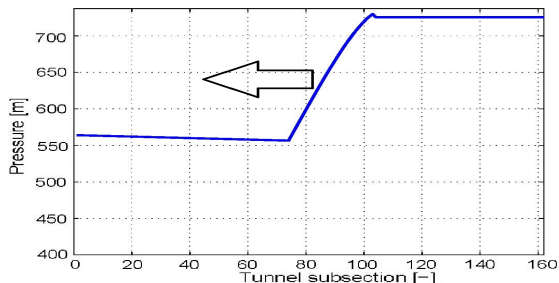


Figure 2.1: Pressure wave front propagating through a pipe

For a conduit with constant speed of sound, this reflection time is

$$T_r = \frac{2L}{a} \quad (2.5)$$

L - Tunnel length

and the pressure oscillation at a given surge location will have a period of

$$T_p = 2T_r = \frac{4L}{a} \quad (2.6)$$

Any periodic regulation of the system with a period close to the natural oscillation frequency given by (2.6) should be avoided whenever possible. However,

for systems containing long tunnels, this might be difficult to rule out. In order to increase predictability, it is common to use surge shafts or surge chambers

2.1.3 Water conduit model

In order to simulate the behaviour of the water conduit, we need to solve equations (2.1) and (2.2). This will be accomplished by the method of characteristics. The method of characteristics is a way of transforming partial differential equations into particular total differential equations, thus making the mathematical model easier to handle.[15]. A brief introduction will be given here. For a more comprehensive investigation, see Appendix D

By linearly combining (2.1) and (2.2) they can be rewritten and separated into

$$\frac{g}{a} \frac{dH}{dt} + \frac{dV}{dt} + \frac{fV|V|}{2D} = 0 \quad \text{for } \frac{dx}{dt} = +a \quad (2.7)$$

$$-\frac{g}{a} \frac{dH}{dt} + \frac{dV}{dt} + \frac{fV|V|}{2D} = 0 \quad \text{for } \frac{dx}{dt} = -a \quad (2.8)$$

By application of a finite difference discretization, (2.7) and (2.8) can be transformed into the algebraic equations called C characteristics

$$C+ : H_P = H_A - B(Q_P - Q_A) - RQ_A|Q_A| \quad (2.9)$$

$$C- : H_P = H_B + B(Q_P - Q_B) + RQ_A|Q_A| \quad (2.10)$$

$$B = a/gA \quad (2.11)$$

$$R = \frac{f\Delta x}{2gDA^2} \quad (2.12)$$

For computational purposes, the equations are rewritten in the following notation. (2.9) and (2.10) become

$$H_{p,i} = C_p - BQ_{p,i} \quad (2.13)$$

$$H_{p,i} = C_m + BQ_{p,i} \quad (2.14)$$

$$C_p = H_{i-1} + Q_{i-1}(B - R|Q_{i-1}|) \quad (2.15)$$

$$C_m = H_{i+1} + Q_{i+1}(B - R|Q_{i+1}|) \quad (2.16)$$

The i subscript indicates the coordinate of the section that is currently being analysed, hence, the $i-1$ and $i+1$ are the sections before and after, respectively.

The only unknowns are the H_p and Q_p variables, that represent head and flow for current time increment in the i -position. For each solution of these equations, one time increment automatically passes.

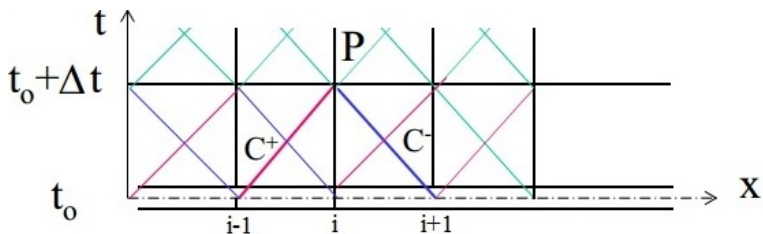


Figure 2.2: Collocated position-time grid where pressure and flow are computed in the same points.

(2.13) and (2.14) are suitable for computing flow Q and piezometric head H for all N interior point of the conduit with length L , given that the following conditions are met;

$$dx = \frac{L}{N} \quad (2.17)$$

$$dt = \frac{dx}{a} \quad (2.18)$$

However, for the boundaries of the conduit, we are missing one of the C characteristics. In addition, for the first iteration we require an initial condition to start the simulation. As for the boundary conditions, they depend completely on the type of interfacing component. Common for all boundary conditions is that either the flow Q_p , or head H_p must be provided and combined with either the C^+ or C^- characteristic. Initial conditions are set from a previously known systemic state.

2.2 Surge control

To be able to control the wave reflection period, one must control the distance to the closest free water surface. This is often achieved by constructing a surge chamber or surge shaft close to the turbine inlet. The distance to the surge control device must be chosen such that the oscillation period is shorter than any predicted periodic regulatory events that the system may experience.

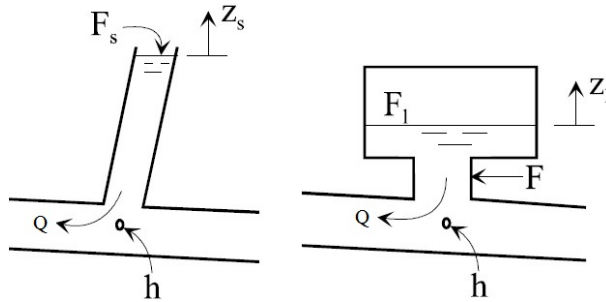


Figure 2.3: Surge shaft and surge chamber [2]

In addition to controlling oscillation frequency, the magnitude of water hammer is also reduced by these devices. The surge shaft counteracts the rising momentum by allowing the water to flow upwards in the shaft, hence dissipating some of the energy to friction and heat as the water rises and allowing the water to slow down over a larger time interval. The surge chamber works in the same manner, however, whereas the surge shaft counteracts the rising pressure by gravity alone, the surge chamber utilizes an additional gas cushion inside the chamber.

In the same way a surge device absorbs water during a negative regulation, it also "feeds" the downstream components during a positive regulation. This allows the water string to accelerate slower, hence further increasing system stability. The shaft alternative is the most common, and by far the least costly. The chamber approach is mostly used when the facility's depth is such that a shaft cannot be constructed. Surge chambers also require good quality bedrock in order to handle the strain that they experience. The system that will be used for verification utilizes a surge chamber, hence this will be the focus for the model.

2.2.1 Surge Chamber model

To simulate the operation of the surge chamber as accurately as possible, both damping provided by the air cushion itself, as well as the loss provided by friction in the entry shaft needs to be accounted for.

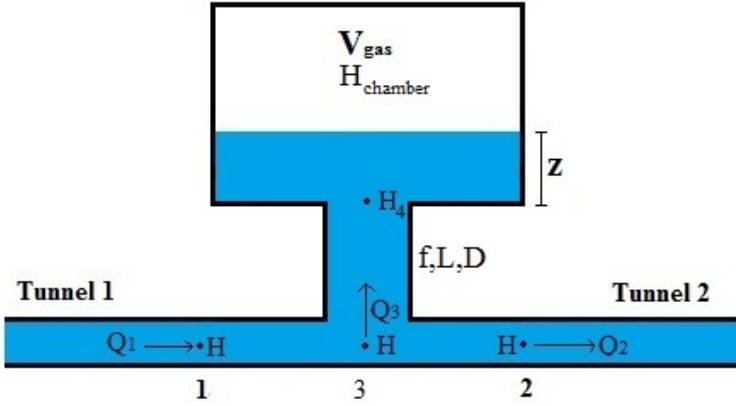


Figure 2.4: Surgechamber model

Using the polytropic relation for a compressible ideal volume of gas, the relation between volume and surge chamber head is given

$$H_{chamber} V_{gas}^n = Const \quad (2.19)$$

Rewriting this equation for a transient change of air volume yields on MOC form[15]

$$H_p (V_{gas} - \frac{Q_{p3} + Q_3}{2} dt)^n = Const \quad (2.20)$$

For the junction between the entry shaft and the penstock, simple mass conservation is applied

$$Q_{p1} = Q_{p3} + Q_{p2} \quad (2.21)$$

The damping provided by the entry shaft is modelled by the use of a lumped inertia model including friction[15]

$$H_p - H_{p,4} = C_1 + C_2 Q_{p,3} \quad (2.22)$$

$$C_2 = \frac{2L_3}{gA_3dt} \quad (2.23)$$

$$C_1 = H_4 - H + \frac{f_{shaft}L_{shaft}}{gD_{shaft}A_{shaft}^2}Q_3|Q_{shaft}| - C_2Q_3 \quad (2.24)$$

Additionally, the two characteristics represented by equations (2.13) and (2.14) is used, forming a solvable system of equations. The flow into the resuming penstock as well as the head in the junction is needed to resume the simulation downstream towards the turbine.

After solving the system, the gas volume must be updated for use in the next iteration

$$V_{gas,new} = V_{gas} - \frac{Q_{p3} + Q_3}{2}dt \quad (2.25)$$

Characteristic properties of the model are surgechamber size and initial gas volume, as well as the properties of the entry shaft.

2.3 Turbine

All components of a hydropower system revolve around the turbine. The turbine converts hydraulic power from the water flowing from the reservoirs into mechanical shaft-power for the generator. 3 types of turbines are in widespread commercial use, Kaplan, Francis and Pelton. The selection of turbine depends mainly on the plant's head and available flow.

Kaplan Used for low head, high flow plants

Pelton Used for high head, low to medium flow plants

Francis Used for medium to high head, medium flow plants

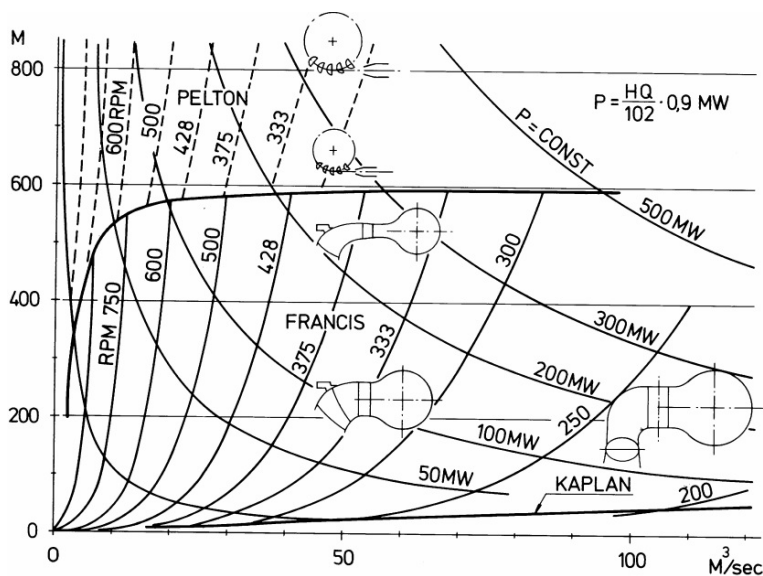


Figure 2.5: Turbine suitability diagram[3]

In this report, an investigation into the use of a model for Francis type turbines will be given. Subsequently, this type of turbine will be the focus in this section. In order to understand the function of a francis unit (and its model) a brief introduction into its four components, spiral casing, guide vanes, runner and draft tube will be provided.

2.3.1 Spiral casing and guide vanes

The water is transferred to the turbine unit, located in the power station, via the fluid conduits. It then enters the spiral casing, the purpose of which is to distribute the waterflow around the runner. The water subsequently passes from the casing and into the runner via the guide vanes. The guide vanes are hydrofoils placed around the spiralcasing. By adjusting the angle of the guide vanes, the water's angle of attack towards the turbine blades(α) are adjusted in order to regulate turbine output torque.

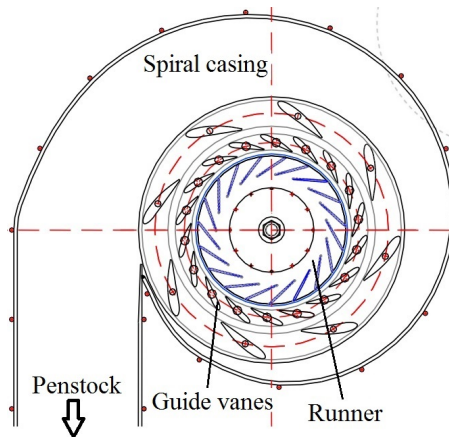


Figure 2.6: Spiral casing with runner[3]

Each turbine design has specific operational parameters that must be met in order to achieve optimum efficiency. This point is based upon the inlet/outlet velocity diagram given in figure 2.7. Factors that influence the velocity components are turbine rotational speed, volumetric flow and guide vane angle. The volumetric flow itself is a function of the guide vane position, however a pressure increase in front of the turbine will also influence the flow.

2.3.2 Runner

The runner is designed in such a way that the water flowing through its curved channels exerts torque and spins the turbine. The properties of each turbine is dependant on its geometry. The turbine characteristics can be described by the one-dimensional Euler equation using the water inlet/outlet water velocities

$$P = \omega T = \rho Q(u_1 c_{u1} - u_2 c_{u2}) \quad (2.26)$$

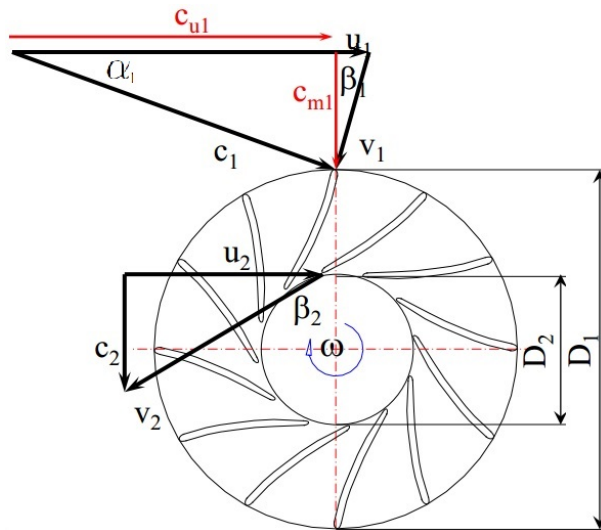


Figure 2.7: Francis inlet/outlet velocity diagram[3]

- P - Turbine output power
- ω - Turbine angular speed
- T - Turbine shaft torque
- u - Peripheral velocity
- c_u - Peripheral velocity component
- c_m - Meridional velocity component
- c - Absolute velocity
- β - Relative angle

The tangential velocities u_1 and u_2 will only change slightly during normal operation as they are a function of the turbine rotational speed which, in turn, is dependant on the relatively constant grid frequency (see section 2.4).

$$U = \omega_{turbine}r \quad (2.27)$$

However, other properties in the triangle will be altered, should α_1 be changed. This is due to both change in the guide vane angle, as well as change in flow through the guide vanes. It can be observed from the triangle that a change of α_1 will result in a change in meridional velocity components, and thus from (2.26), a change in torque.

2.3.3 Self governing

For fully submerged turbines such as Francis type, a phenomenon called self-governing occurs. This occurs due to flow in the turbine channels being dependant on the rotational speed. When the generator is disconnected from the grid, the runner is allowed to rotate faster than its design parameters. This will result in a throttling of the turbine due to increased centripetal force acting on the water as it flows through the runner. This results in lower efficiency, and any further increase in rotational speed will be reduced. This increases stability during load rejections.

2.3.4 Draft tube

The draft tube is a conical pipe directing the water away from the turbine after it as passed through the runner. The purpose of the draft tube is to convert residual kinetic energy in the spent water back to pressure energy, in order to increase the pressure differential over the turbine, hence increasing efficiency.

2.3.5 Turbine Losses

A modern water turbine is a very efficient machine, however it is not able to extract all the energy from the flowing water. There are several sources of loss that influence the overall efficiency.

Friction losses occur due to contact friction between rotating and stationary parts, as well as friction from the water enclosing the turbine. These losses act as a resistance against rotation.

Losses due to undesirable inflow conditions occurs when the turbine is operating outside its design parameters. The velocity triangle, described in section 2.3.2 will then be outside optimum conditions.

Draft tube loss occurs as a result of undesirable flow angle out of the runner, causing swirl. Due to this swirl, the draft tube fails to regenerate some kinetic energy from the flow. Both draft tube loss and inflow angle losses are caused by flow angles being out of optimum design point.

Viscous loss occurs throughout the turbine in the same way as in pipes.

Leakage loss is a reduction in output power due to the loss of water mass. This usually occurs as the water is flowing from the spiral casing into the runner, by leakage via the small gap between them.

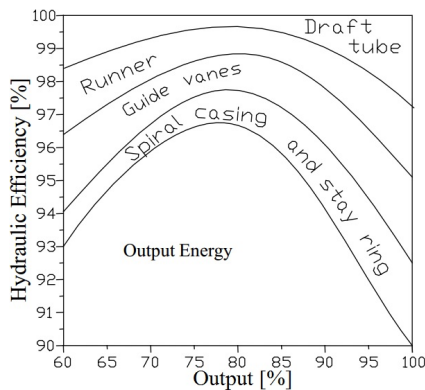


Figure 2.8: The sum of all losses creates the efficiency diagram[3].

2.3.6 Turbine model

The conduit boundary conditions represented by the turbine is the main challenge in the simulation. Creating a model from scratch is beyond the scope of this thesis (and competence of the author), hence a model suggested by Nielsen[10][9] will be implemented. A brief description is given.

The turbine supplies torque to the generator. This torque can be modelled as

$$T_{turbine} = \tilde{q}(\tilde{m}_s - \psi\tilde{\omega})\eta_{hydraulic} - R_m\tilde{\omega}^2 \quad (2.28)$$

The dimensionless torque \tilde{m}_s is defined as

$$\tilde{m}_s = \xi \frac{\tilde{q}}{\kappa} (\cos(\alpha_1) + \tan(\alpha_{1,R})\sin(\alpha_1)) \quad (2.29)$$

where

$$\xi = \frac{\psi + 1}{\cos(\alpha_{1,R})} \quad (2.30)$$

- \tilde{q} - Dimensionless turbine flow
- ψ - Pressure number
- $\tilde{\omega}$ - Dimensionless turbine rotational speed
- R_m - Loss constant (mechanical/water friction)

The equation for the turbine pressure differential attaches the turbine-model to the water conduit. To avoid a overdetermined system, this is given on MOC form, meaning that the turbine head is determined via its flow and one C-characteristic.

$$C_p - BQ_R\tilde{q} = H_s + H_R \frac{1}{1 + \sigma} \left(\frac{\tilde{q}^2}{\kappa} + \sigma\tilde{\omega}^2 \right) \quad (2.31)$$

The inlet angle α_1 is dependant on the turbine opening κ

$$\kappa = \frac{\sin(\alpha_1)}{\sin(\alpha_{1,R})} \quad (2.32)$$

- κ - Turbine degree of opening
- H_s - Turbine submergence head

The self-governing parameter σ defines the efficiency loss when the turbine is rotating faster than its rated speed, given as

$$\sigma = -\frac{1 - \psi(1 - R_f) - 2R_m}{2R_f \frac{1+R_m}{1-R_f} - \psi(1 - R_f) - 1 - 2R_m} \quad (2.33)$$

R_f - Viscous loss constant

To simulate dynamic behaviour, accurate loss modelling is needed. Modelled losses are divided into three categories, viscous, frictional and angle losses. The hydraulic efficiency is expressed as

$$\eta_{hydraulic} = 1 - \frac{\Delta h}{h_R} \quad (2.34)$$

and

$$\Delta h = \overbrace{R_f \tilde{q}}^{\text{Viscous loss}} + \overbrace{(R_c + R_d)(\tilde{q} - \tilde{q}_c)}^{\text{Inflow angle loss}} \quad (2.35)$$

R_d - Draft tube loss constant

R_c - Angle loss constant

The reduced flow \tilde{q}_c represents what the flow should have been at an optimum angle for the current operation condition, expressed as

$$\tilde{q}_c = \tilde{\omega} \frac{1 + \cot(\alpha_{1,R}) \tan(\beta_{1,R})}{1 + \cot(\alpha_1) \tan(\beta_{1,R})} \quad (2.36)$$

The constants R_c and R_d is combined into the constant R_a . The equations above will be used to extract the hydraulic parameters $\tilde{q}, \omega, \kappa$, and via \tilde{q} , the head H . The simulation will use a general Euler turbine, hence all properties regarding geometry and runner flow speed is not necessarily accurate for the real turbine. However, all other properties such as the transient head, volumetric flow, power etc will hopefully be a good representation of the real unit.

2.4 Generator

The runner is connected to the generator via a drive shaft. The shaft rotates the generator rotor which is located inside the generator stator. Several types of generators exist, and may appear quite dissimilar in their theoretical way of operating. However, for our modelling purposes, simple considerations are adequate.

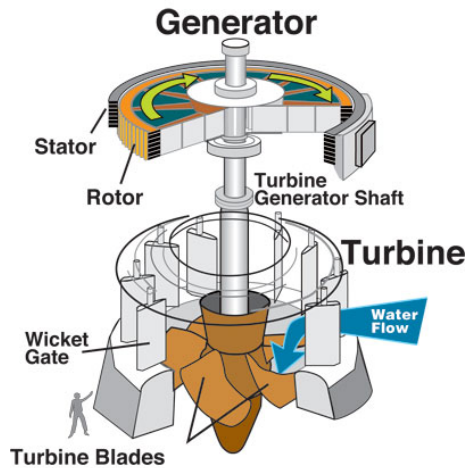


Figure 2.9: Turbine with generator

2.4.1 Elementary concepts

Faradays law of induction states that a change in electromagnetic flux will induce an electric transient potential known as voltage.

$$e = -\frac{d\lambda}{dt} \quad (2.37)$$

where

λ - Magnetic flux

This is achieved by rotating windings located in the rotor through a magnetic field created by magnets in the stator. This creates a cyclic variation in the

magnetic flux λ , and thus according to (2.37) induces the alternating voltage e .

The generator needs to generate an alternating voltage signal with a frequency specified by grid-users, usually a small interval around 50 or 60 hz (see section 2.5). In order to achieve this, the generator rotor needs to have the correct amount of rotor poles with regards to the turbine optimal rotational speed. For a 2-pole generator, the voltage completes one period per revolution of the rotor. The voltage angular frequency for steady-state operation is then described by

$$\omega_{grid} = \omega_{generator} = \frac{P}{2}\omega_t \quad (2.38)$$

where

- ω_{grid} - Grid angular frequency
- P - Generator poles
- ω_t - Turbine angular frequency

This means that the generator must yield a variable power output at a constant rotational speed. It must also operate within a reasonably constant voltage. The output power (and torque) is then a function of the output current.

$$P_{electric} = \omega_{grid}T = EI \quad (2.39)$$

The output is increased by adjusting the rotor magnetization current. When the generator is producing power at a steady-state condition, the rotor will rotate at an angular displacement located in front of the synchronous reference frame of the stator.

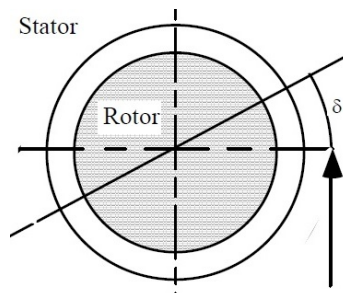


Figure 2.10: Magnetic displacement angle between generator rotor and stator

This can be viewed as the rotor "pulling" the magnetic field along with the rotation. This angle is a function of the generator output, the larger the output, the larger the displacement. Should either the output power or grid frequency change, so will the magnetic displacement angle, thus allowing the turbine to accelerate the rotor slightly despite being grid-connected[4].

Shifting the synchronous machine power angle requires torque. This will act as a magnetic spring that resists sudden changes in rotational speed, hence acting in the direction opposite of rotational acceleration. All of these factors must be accounted for in the simulation model.

2.4.2 Generator model

Faraday's law(2.37) states that generator voltage output is dependant on the change in magnetic field strength. The magnetic field strength is a complex variable for a rotating machine and represents informaton that is not needed for the purposes of this investigation. Rewriting

$$E = K_m \omega_{grid} \quad (2.40)$$

where

K_m - Magnetic flux variable

The variable K_m describes the flux-linkage in the generator such that the angular velocity can be used directly as the time-derivative term.

The torque needed to run the generator is primarily dependant on the magnetic field from the stator and the current generated in rotor[4], thus

$$T_{generator} = K_m I \cos(\phi) \quad (2.41)$$

where

I - Generator current

ϕ - Grid powerangle

As the electrical frequency of the grid is set externally, the magnetic angular displacement must be

$$\frac{d\delta}{dt} = \frac{P}{2} \omega_{turbine} - \omega_{grid} \quad (2.42)$$

The torque needed to shift it is described linearly as

$$T_{damping} = m_d \frac{d\delta}{dt} \quad (2.43)$$

where

- $T_{damping}$ - Torque due to change in synchronous machine power angle
- m_d - Magnetic damping constant
- δ - Synchronous machine power angle

When the angle has stabilized, the new torque required to turn the generator is approximated as

$$\frac{T_g}{T_{g,max}} = \frac{\sin(\delta)}{\sin(\delta_{max})} \quad (2.44)$$

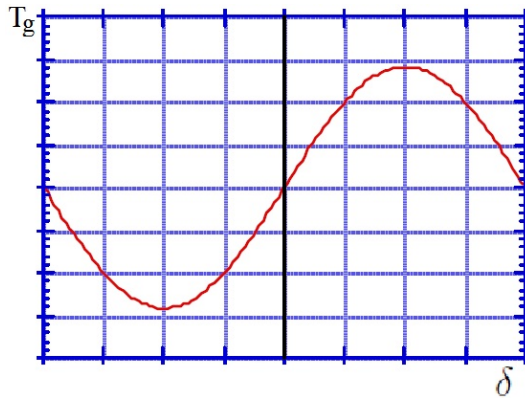


Figure 2.11: Generator torque as a function of displacement angle

2.5 Power system and grid

A power plant has two tasks. The first is to supply energy to the clients attached to the system via the grid. The other is to aid in overall grid stability. In this term, stability is focused around grid frequency and voltage.

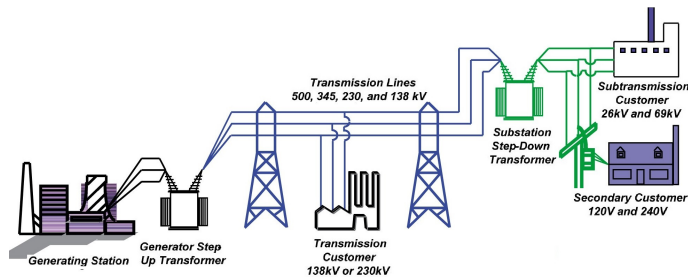


Figure 2.12: Power system illustration

2.5.1 Frequency and flywheel mass

All components and appliances connected to the grid is designed to operate at a specific frequency or set of frequencies, thus it must not be allowed to significantly drop or increase. In the Norwegian grid, variations of up to $\pm 100\text{mHz}$ are allowed without initiating active regulation. Variations in the frequency are caused by changes in the supply/demand balance. This can be explained by the combined rotating flywheel mass of all synchronous rotating units.

All rotating units have mass attached to them, most is due to the machine components themselves. However, extra flywheel mass is also added. While rotating, this mass can store large amounts of energy, hence acting as a buffer. When the energy demand increases, energy is drained from this mass and actually allows the units to deliver more energy than is actually produced for a short period of time. As a consequence, the collective rotational speed of all units will drop and as observed from equation (2.38), this will result in a drop in frequency. To counteract this, some units will need to increase production in order to meet the increased demand as well as to "recharge" the drained mass.

2.5.2 Load distribution and permanent speed droop

When the load changes, some units are more suited to handle this variation than others. Examples are thermal plants versus hydropower plants. Thermal plants are very slow, and does not change load easily. On the other hand, hydropower plants can change load almost instantly and are therefore more suited to keep grid stability. To determine which plant will handle changes in load, the governors that regulate generator ouput has a property called "permanent speed droop" (see section 2.6 for more information)

This property sets a slope between variations in load versus frequency, illustrated in figure 2.13.

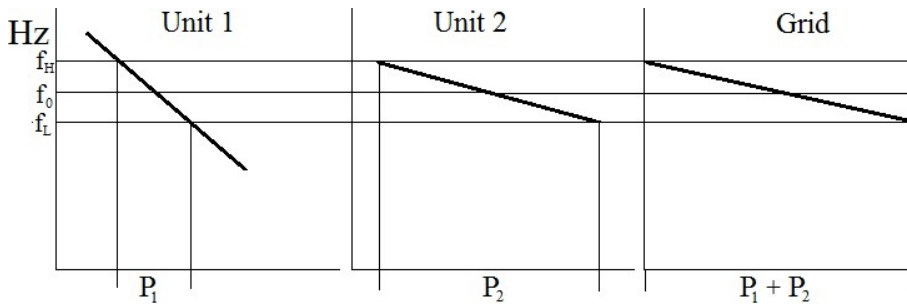


Figure 2.13: Speed droop and power distribution line for two units creating their own grid

Setting a steep load variation line will mean the plant output is independent of grid frequency (typical of large thermal plants), and a flat line gives large load variations with change in frequency (typical of agile hydropower plants). The sum of all responses will set the total grid frequency as a function of load demand.

2.5.3 Grid modelling

An actual power grid is inherently complex and an advanced model is way beyond the scope of this thesis. Hence, the grid will be represented by a single node combined with a simple Thèvenin equivalent.

The load is subsequently assumed ohmic, thus

$$\phi = 0 \Rightarrow pf = \cos(\phi) = 1 \quad (2.45)$$

where

pf - Grid power factor

The grid voltage is determined from the attached grid load and the supplied current from the connected units, hence from Ohm's law

$$E_{grid} = R_{grid} \sum_{i=1}^n I_i \quad (2.46)$$

The grid can be simulated in two modes. The first mode is that the grid is assumed static, meaning simulated units are unable to influence grid frequency. This is usually the case with all but the largest units in most grids. In this scenario, the grid frequency is an input to the simulation. To simulate load variations, the frequency is simply altered to the conditions one wants to simulate.

The second mode is such that the simulated units themselves determine the grid frequency. This might be valid if one is simulating large units attached to decentralized grids. In this case, the frequency is set by

$$\omega_{grid} = \frac{E_{grid}}{K_m} \quad (2.47)$$

The easiest way to implement this is to input the desired expression of grid frequency directly into equation (2.42)

2.6 Governing

In order to meet the demands of the grid, both the turbine and generator needs to be continuously regulated and controlled. This is achieved by using governors that monitor key parameters and, when the situation dictates, takes action in order to maintain the desired operational conditions. The two components are regulated in different ways

The turbine is regulated by adjusting the guide vanes and hence the opening degree κ . The parameter that determines if regulating is required is the turbine rotational speed.

The generator is regulated by adjusting the magnetic flux constant K_m , in order to regulate output voltage toward the grid.

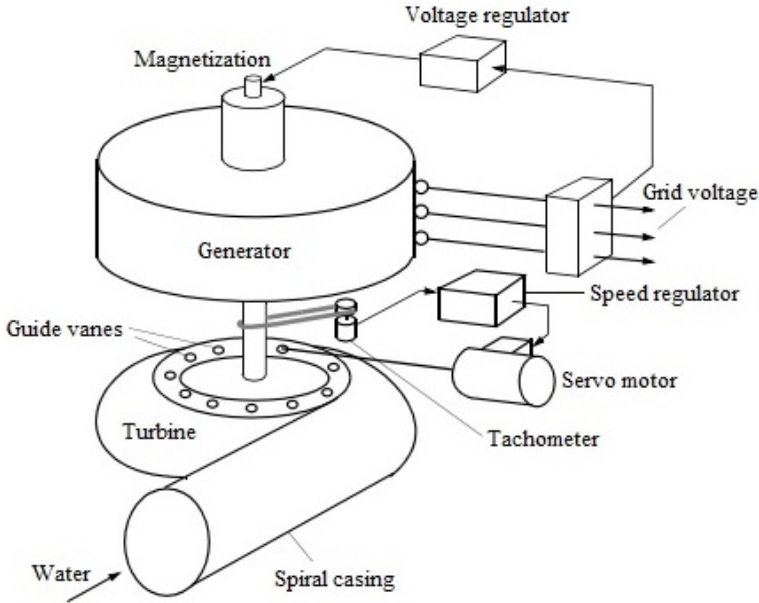


Figure 2.14: Turbine assembly with regulators[1]

This can be achieved in various ways, however the most common regulator is the PI or PID controller.

2.6.1 PID regulator

The Proportional Integral Derivative regulator is regulating process, usually formulated

$$u(t) = \overbrace{K_P D(t)}^{\text{Proportional}} + \overbrace{K_i \int_0^t D(\tau) d\tau}^{\text{Integral}} + \overbrace{K_d \frac{d}{dt} D(t)}^{\text{Derivative}} \quad (2.48)$$

where

- $u(t)$ - Output signal
- $D(t)$ - Deviation from desired operating point
- K_p - Proportional gain
- K_i - Integral gain
- K_d - Derivative gain

The output signal is a superposition of the three terms

Proportional uses the deviation D along with the gain K_p to calculate control signal output. The contribution from the proportional term is only dependant on the magnitude of deviation, hence there will always be a small steady-state deviation called droop.

Integral corrects for droop by accounting for duration of previous deviation, in addition to the magnitude. The integral contribution thus increases as long as a deviation exist. In this way the integral term accounts for accumulated deviation, multiplies this by the integral gain K_i , then adds this to the proportional contribution.

Derivative calculates the rate of change, or slope of the deviation, thus anticipating future deviation. This slope is then multiplied by the derivative gain K_d and added to the other terms. The derivative gain is often small (or even zero) as this term is highly sensitive towards measurement noise.

The gain constans are often expressed in terms of time constants

$$K_p = \frac{1}{\delta_t} \tag{2.49}$$

$$K_i = \frac{1}{\delta_b T_i} \tag{2.50}$$

where

- δ_t - Transient speed droop
- δ_b - Permanent speed droop
- T_i - Integration time constant

The gain settings (values of K_p, K_i, K_d) may differ from process to process, and must be tuned accordingly. The PID regulator can be transformed into the simpler PI regulator by setting the derivative gain, K_d , to 0.

2.6.2 Governor modelling

To make the two governors easier to program and implement, the integral-term is removed by using the differentiated form of (2.48) without the D-term.

The turbine needs a regulator that governs RPM via the guidevanes (κ).

$$\frac{dc}{dt} = \frac{\kappa_{ref}}{T_k} \left[-\frac{1}{\delta_t} \frac{1}{n_{ref}} \frac{dn}{dt} + \frac{1}{\delta_t T_d} \left(\frac{n_{ref} - n}{n_{ref}} \right) - \frac{(\delta_b T_k + \delta_t T_d)}{\delta_t T_d} c - \frac{\delta_b}{\delta_t T_d} (\kappa_{ref} - \kappa) \right] \quad (2.51)$$

where

- c - Servo motor velocity
- n - Speed of rotation
- δ_t - Transient speed droop
- δ_b - Permanent speed droop
- T_d - Integration time
- T_K - Servo motor time constant

Note that the terms containing the permanent speed droop defines the allowed deviation from a set reference. This will create the load distribution line described in section 2.5.2. The servo time constant defines how fast the servo can respond.

The generator regulator governs output grid voltage via the magnetization constant K_m

$$\frac{d(K_m)}{dt} = -\frac{1}{\delta_{tg} E_{ref}} \frac{dE}{dt} + \frac{1}{\delta_{tg} T_{dg} E_{ref}} (E_{ref} - E + \frac{1}{\delta_{bg} I_{ref}} (I - I_{ref})) \quad (2.52)$$

These equations need to be integrated before being coupled with the remaining equations. For more information about the derivation of the regulator equations, the reader is referred to [11]

2.7 Turbine/generator coupling

The turbine unit is connected to the water conduit as well as the generator, which in turn is connected to the electrical grid. The equations that model each component have now been explained, as well as the link between the grid and generator. However, a link between the turbine and generator is needed to complete the system. This is achieved through a simple torque-balance differential equation describing rotational acceleration

$$J \frac{d\omega_t}{dt} = T_{source} - T_{drain} = T_{turbine} - T_{generator} - T_{damping} \quad (2.53)$$

substitution using equations (2.28), (2.41) and (2.43) and transforming all terms to dimensionless form

$$T_a \frac{d\omega_t}{dt} = \tilde{q}(\tilde{m}_s - \psi\tilde{\omega}) - R_m\tilde{\omega} - \frac{K_m I}{T_{generator,R}} - m_d \frac{d\delta}{dt} \quad (2.54)$$

where

$$T_a = J \frac{\omega_R^2}{P_R} \quad (2.55)$$

and

- T_a - Inertia time constant
- J - Polar moment of inertia
- P - Rated turbine power

This completes the system of equations. This means that the complete system, from power grid to water conduit is described by equations (2.31), (2.42), (2.40), (2.51), (2.52), (2.54) and Ohm's law for the generator current. The pressure fluctuations in the conduit is solved using (2.13) and (2.14), and the surge chamber is modelled according to section 2.2.1

Chapter 3

Model implementation

By using the equations stated in chapter 2, a MATLAB model was created, along with an attached graphical user interface (GUI). A brief overview of the program will be given, in order to provide the reader with a general understanding of the method. The code for the program's main components can be found in appendix A. The GUI source code itself is several thousand lines long, therefore not attached, however it can be viewed electronically.

3.1 General description

The program is created with the intention of letting the user simulate both load variations and load rejections. Two units are supported from the GUI, however more can be added programatically. The GUI allows the user to input characteristic data for the the two turbines and generators, as well as for the tunnel network. When the simulation is completed, all relevant data is sent back to the GUI for plotting. The GUI has six active tabs

Simulation Sets basic low-level simulation parameters such as simulation time and time increment (dt).

Conduits Allows the user to adjust reservoir head, wave propagation speed in water and tunnel-wall friction factors.

Turbine Settings for turbine and turbine governor.

Generator Settings for generator and generator governor.

Events Allows the user to create simulation event schedule.

Results Available when the simulation is completed. The user may select the desired data and the data is plotted to the GUI or external window for export.

The program operates according to the basic flow diagram below, indicating the main components of the algorithm.

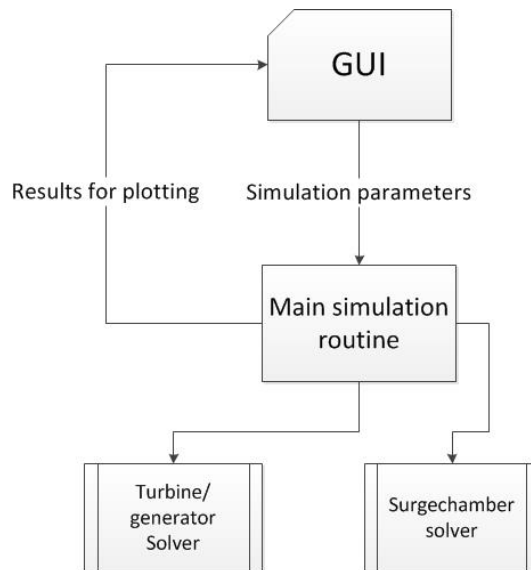


Figure 3.1: Program overview

The GUI handles basic user interaction, and it is possible to run simulations without manually altering the source-code. However, it is beyond the scope of this project to implement every conceivable function. As a result, advanced use requires some programming skills.

The main routine imports and creates simulation variables, handles time-settings and calculates waterway properties. An overview flow chart is given in figure 3.1.

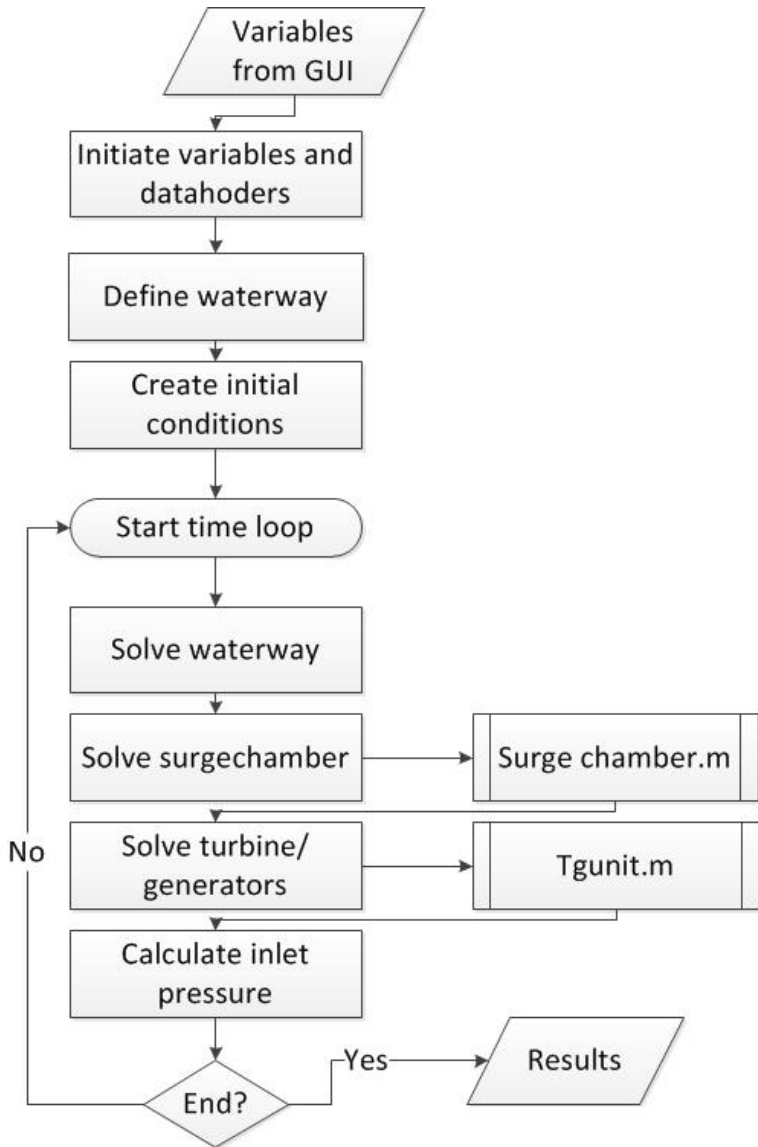


Figure 3.2: Simulation routine flowchart

The main routine uses several auxiliary functions, the most prominent being solver for the surge chamber and turbine/generator units. The latter is the workhorse of the program, solving all equations that simulates dynamic behaviour of the units. It solves 5 differential equations on the fly using a forward Euler scheme, as well as 4 algebraic ones.

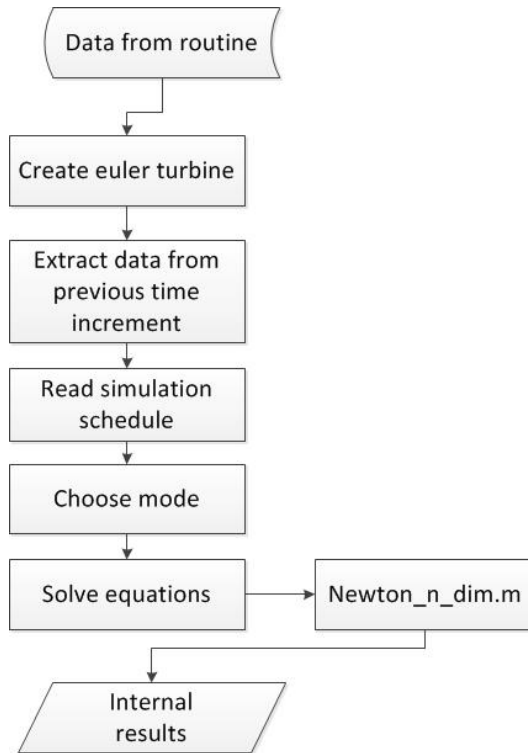


Figure 3.3: Program overview

These equations are discussed in chapter 1, and solved using a symbolic Newton-Raphson method. For more information, view the code in appendix A

3.2 Input/Output

Required input data in most of the tabs are intuitive. However, a list of input for the turbine and generator tab is given

Table 3.1: GUI input for turbine and generator

Turbine	Generator
Runner frictional loss	Output
Transient speed droop	Transient speed droop
Permanent speed droop	Permanent speed droop
Integration time	Integration time
Rated head	Rated voltage
	Rated angle displacement

Note that not all inputs can be set via the GUI, some must be set in the source code.

The program returns the following results for for each turbine/generator unit. These are vectors with time increment number as index.

Table 3.2: Output for simulated turbine/generator units

Turbine	Generator
Flow	Power
Rotational speed	Magnetic constant
Guide vane position	Magnetic angle
Servo acceleration	Voltage
	Current

The pressure and flow for each point in the waterway for each time increment is also returned.

3.3 Expandability

The author tried to have expandability in mind when developing the program. This must be done in the source code, not the GUI. Expanding system to involve more turbine/generator units can be done by expanding the main routine in the following way

- Define additional dataholder for the new unit
- Add the new unit in the code block for finding steady state efficiency, hence initiating it
- Add the new unit in the main time loop, right after the other units (this is assumed it is in the same node)

The same procedure can be done for adding a surge chamber.

Altering the waterway must be done in the first part of the main routine, where the grid is defined.

Chapter 4

Model calibration and discussion

The implemented model has several parameters that are specific for the turbine that needs to be simulated. In order to accurately simulate a system, the turbine/generator-model, as well as the waterway needs to be calibrated towards the desired system. As a step towards verifying the accuracy for the model, it will be calibrated and tested towards known measurements of the Driva hydropower system operated by TrønderEnergi Kraft AS.

4.1 The Driva system

The Driva power plant is equipped with two Francis units and Europe's first air cushion surge chamber. The conduit system is relatively complex, with over 30 km of tunnels, several inflow shafts, and a pump station pumping from bi-reservoir Ångårdsvatn into Dalsvatn. The main reservoir is Gjevilvatnet with 15m manouvering capability and a capacity of 280 Mm^3 .^[7] (See appendix E for more information)

Table 4.1: The general system has the following properties

Reservoir HRV	Reservoir LRV	Tail water head
660.8 m	645.8 m	91 m

Table 4.2: The two installed units have the following properties at peak efficiency[6] [13]

Unit nr	Efficiency	Flow	Head	Power	RPM	Voltage
1	93.95%	$13.12 \frac{m^3}{s}$	540 m	65.37 MW	600 rpm	11 kV
2	94.65%	$13.81 \frac{m^3}{s}$	540 m	69.50 MW	600 rpm	11 kV

The generator efficiency is assumed to be a constant 98.2% during normal operation, being an estimated average of the measured curve[6]. Unit one has a bypass valve installed.

Available background data for the plant are

- Load rejection reports [14] [5]
- Efficiency measurements (Confidential, hence these documents are not attached)
- Plant system stability analysis [7]

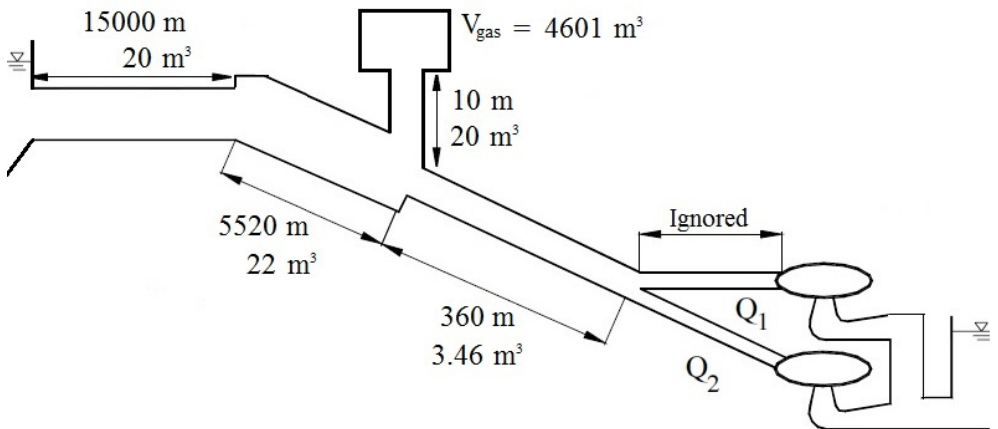


Figure 4.1: Input geometry for the simulation

The loss coefficients described in section 2.3.5 and 2.3.6 was calibrated in the manner described below

4.2 Tunnel frictional loss coefficients

Stream intakes were ignored in the implementation of the conduit system, leaving just the headrace tunnel and penstock. The tunnel was divided into the following sections[6]. Note that the section lengths were rounded to meet dx-requirements for the method of characteristics.

Table 4.3: Waterway division

Section nr	Area	Length	Surface type
1	20 m^2	15 km	Blasted rock
2	22 m^2	5.52 km	Blasted rock
3	4.15 m^2	0.36 km	Concrete

The tunnel friction coefficients were calibrated by assuming a reservoir head of

$$H_{reservoir} = H_{LRV} + \frac{H_{HRV} - H_{LRV}}{2} \quad (4.1)$$

and setting the nominal turbine head of 540 meters as target. The combined flow was set to the sum of nominal flow values. The friction factors for the penstock and general tunnels where then adjusted to match the measured tunnel head differential. The friction in the blasted tunnel was assumed to be roughly five times the value of the concrete lined penstock. The estimated result was then compared to measurements performed on the facility in 1991 [12].

Table 4.4: Calibrated waterway frictional loss coefficients

Section	Simulation coefficient	Measured coefficient	Deviation
Tunnel	0.0467	0.02668	75.03%
Penstock	0.0102	0.00569	79.26%

The calibrated friction coefficients are about 75 % larger than measured. This may be due to incomplete system model (not all tunnels accounted for) and that the friction model does not account for impact losses in the conduit. Deviation in this area was expected, as the tunnel loss simulation is very basic.

4.3 Turbine time constants

The combined rotor inertia for each of the two units are unknown, and must be estimated. This was achieved using the transient rpm-plot during a rejection. The initial slope (right after decoupling the generator) was measured, and then extrapolated to where the line would have intersected the $2N_{ref}$ line. The inertia was then found by using (2.55) with the measured T_a and power output during the rejection. The nominal value of T_a is found by using the inertia and nominal power output. As expected, the newer unit two is lighter.

Table 4.5: Inertia and time constants

Unit	J	T_a
1	118667	7.16
2	82070	4.662

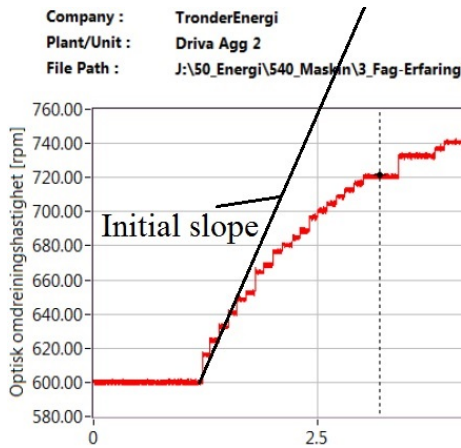


Figure 4.2: Example of measurement of acceleration time constant

4.4 Turbine frictional loss coefficients

Turbine frictional constant R_m was calibrated using load rejection data for the two units. Using the rpm-plot, the slope of declining rotational speed was found after the turbine was closed. The model frictional loss constant is increased until the simulated runaway-speed slope is similar to the results from the report.

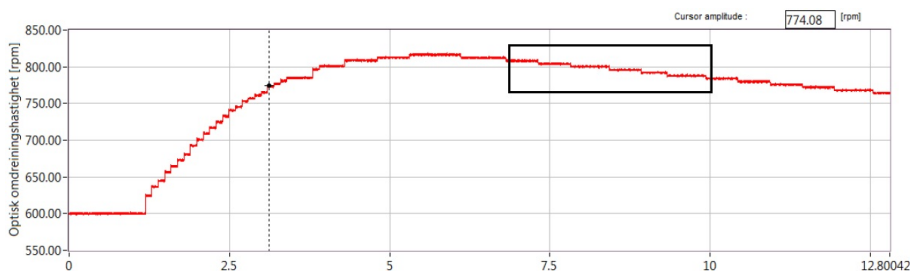


Figure 4.3: Declining rpm slope for calibration

Table 4.6: Calibrated turbine/generator frictional loss coefficients

Unit nr	Measured slope	Simulated slope	R_m
1	$-6.6 \frac{rpm}{s}$	-6.41	0.04
2	$-10.5 \frac{rpm}{s}$	- 10.44 $\frac{rpm}{s}$	0.042

As expected, the frictional loss coefficients are very similar, as the assemblies (except the turbine runners) are identical. However, the author suspects that these coefficients are slightly overestimated. This is due to the loss of the viscous loss term as the turbine is closed (flow is zero in (2.28)), despite that the turbine is still submerged in water and spinning at high rpm. This, in turn, will cause an underestimation of the hydraulic loss constants.

4.5 Turbine hydraulic losses

The calibration of the hydraulic loss constants R_f and R_a is adjusted so that the turbine meets the nominal efficiency. The hydraulic loss is modelled according to (2.35). At optimum efficiency, the loss related to undesirable inflow angles are

zero and the friction loss coefficient already calibrated, thus the only parameter left to adjust is R_f . Calibrated values are given below.

Table 4.7: Calibrated turbine viscous loss coefficients

Unit nr	Reported efficiency	Simulated efficiency	R_f	$\eta_{hydraulic}$
1	93.95%	93.95%	0.0205	97.95%
2	94.65%	94.65%	0.01135	98.87%

As commented earlier, the hydraulic efficiencies are overestimated.

The losses due to inefficient flow angles was calibrated by choosing a point on the efficiency curve other than that of optimum. The following points were chosen

Table 4.8: Calibrated turbine angle loss coefficients

Unit nr	Turbine power	Reported efficiency	Model efficiency	R_a	$\eta_{hydraulic}$
1	84.89	93.24%	96.8%	0.6	96.22%
2	85	94.27%	97.5%	0.6	98.17%

As can be observed from table 4.8, the target efficiency was not reached. At high values of R_a , the model became unstable and often stalled. The term $q - q_c$ might be unsuited for use at small inflow angles (Euler-turbine used as a base in the turbine simulation has an inflow angle of 3.4 degrees) For real turbines, det angle $\alpha_{1,R}$ is higher. Other factors that might add to the discrepancy might be underestimation of the viscous loss constant. As a consequence of this, the models efficiency will not be correct at off-design conditions. This will underestimate flow slightly, thus underestimating surge pressure during rejections.

The reason for the discrepancy in efficiency was discovered. It turns out the author neglected to account for the loss in efficiency given by the Euler equation. The last term in equation (2.35) is to correct for viscous angle loss that must then be added to the angle loss given by Euler. The author did not have time to correct for this, as this would have meant reconducting all simulations. This does not significantly change the results or conclusions presented in this thesis.

Chapter 5

Results and discussion

Various simulations were performed in an attempt to verify the validity of the model.

1. Load rejections were simulated with the intent of verifying pressure surges in the waterway as well as turbine behaviour of both units during the rejection. The results were compared with measurements of penstock pressure and turbine rotational speed during load rejections trials of the real system. The author sees no point in performing load rejections for a wide variety power output levels for each unit. It is of interest to verify the model for worst-case scenarios, hence rejections with high power outputs and volumetric flow rates.
2. Instant turbine closures were simulated and compared to analytical Joukowski surge (2.3) and ideal pressure reflection times (2.6).
3. Changes in grid load represented by variations in the grid frequency were simulated, while the units were running at nominal load. The intent was to observe the general behaviour of both turbines, and their responses towards both fast drops in frequency and periodic fluctuations. The author does not have access to measurement data for these scenarios, hence verification will be on the background of general behaviour only.

5.1 Load Rejection

Load rejections were simulated for both units. These were performed one at a time, and subsequently compared to the results documented in [14] and [5]. Data for these measured rejections can be found in appendix F.

5.1.1 Rejection unit two over 5.9s from 81.16 MW

Table 5.1: Simulated rejection data for unit two compared to measured data

Type	Simulated	Measured	Deviation
Increase to runaway speed	268.1 rpm	217 rpm	23.55%
Surge pressure increase	68.6 m	77 m	10.9 %

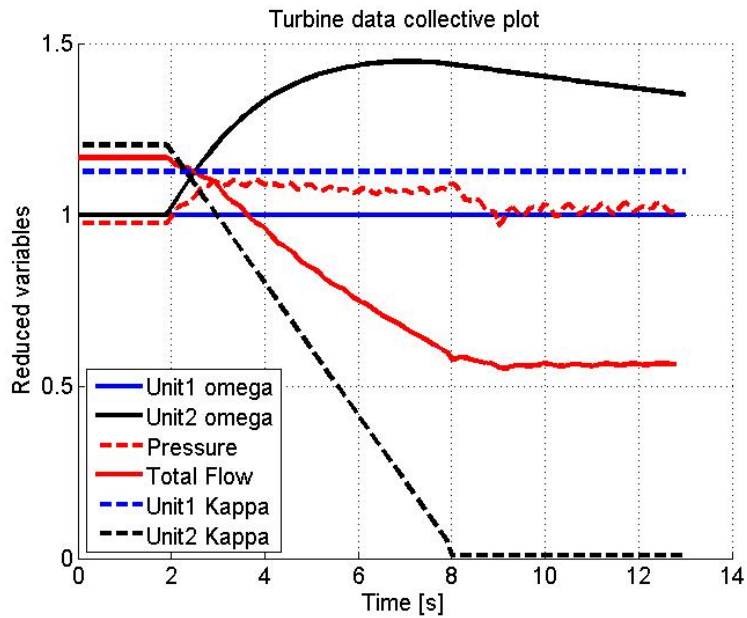


Figure 5.1: System response during rejection of unit two

As can be observed from table 5.1 the simulations overestimate the turbine runaway speed. Some overshoot was expected as there were some difficulties towards obtaining correct model efficiency by the implemented loss model. Additionally, the inertia of the unit was determined graphically, and hence represents a potential source of error. As an initial estimate, the value is seems reasonable.

The surge pressure rise was underestimated by 10.9%. The author wishes to point out that although the reported max pressure is 601 meters, observation of the graph in appendix F indicates that the pressure is generally around 597 meters. This brings the deviation down to 5.7 %. Additionally, the overestimation in efficiency (described in the previous chapter), will cause underestimation of the surge. Overall, the results are considered fairly accurate. This inspires confidence in the models ability to both predict flow through the units at off-design as well as the ability to predict pressure surge magnitude.

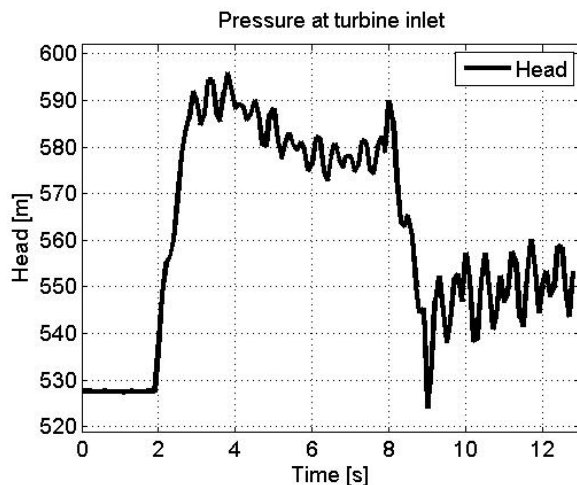


Figure 5.2: Pressure transient during load rejection of unit two

The initial pressure before rejection in front of the turbine was 527.5 meters. Compared to the measured 524 meters, it becomes apparent that the linear frictional loss model is unable to account for all losses in the waterway, when the system state is other than that for which it was calibrated.

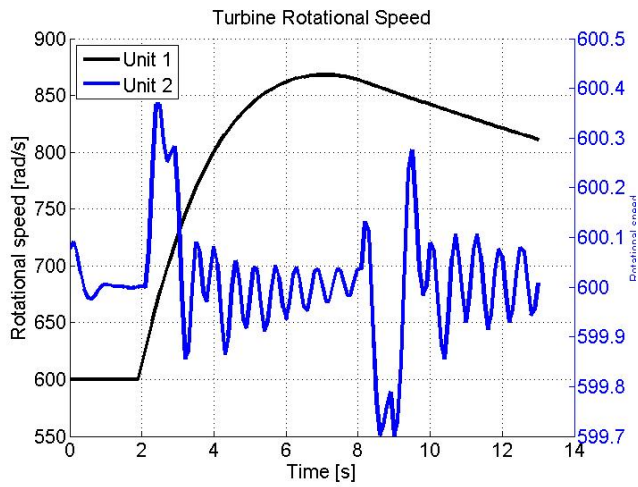


Figure 5.3: Rotational speeds during rejection of unit two

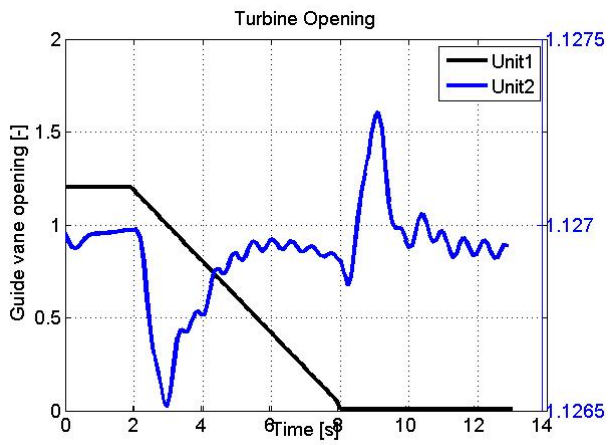


Figure 5.4: Guide vane position during rejection of unit two

Rotational speeds and opening degree is given in figures 5.3 and 5.4. Note the dual y axis. The simulation starts with a slight deviation from the reference 600 rpm. This is believed to be rounding error. The model quickly stabilizes. As the initial pressure surge occurs, the pressure differential over, the still operational, unit 1 increases. This results in larger output and a slight acceleration of the rotor as the generator angle changes (see section 2.4). The regulator almost stabilizes the rotational speed by the time the pressure drops back down. An opposite response is then observed. This is expected behaviour and further builds confidence around the model.

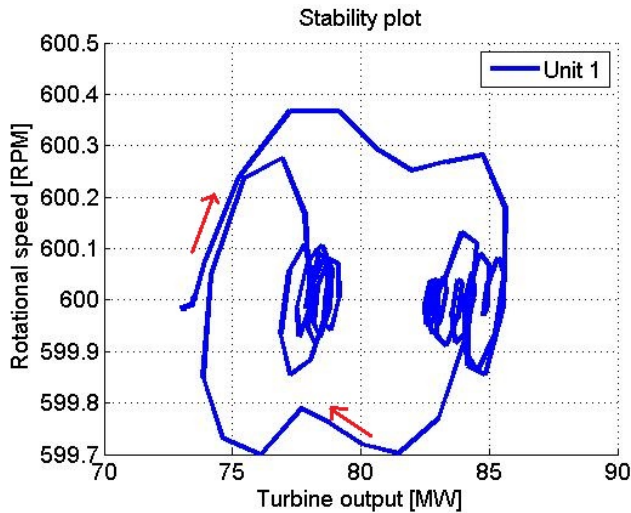


Figure 5.5: Shaft output of unit one during rejection of unit two

Figure 5.10 shows how the transient turbine output as the rejection occurs. The initial output as well as the regulation characteristic around the "high pressure" and "low pressure" conditions are clearly visible.

5.1.2 Rejection unit one over 8.4s from 78.12 MW

Table 5.2: Rejection data for unit one compared to measured data

Type	Simulated	Measured	Deviation
Max rotational speed	249.2	211	18.10%
Surge pressure increase	57.2	49	16.67%

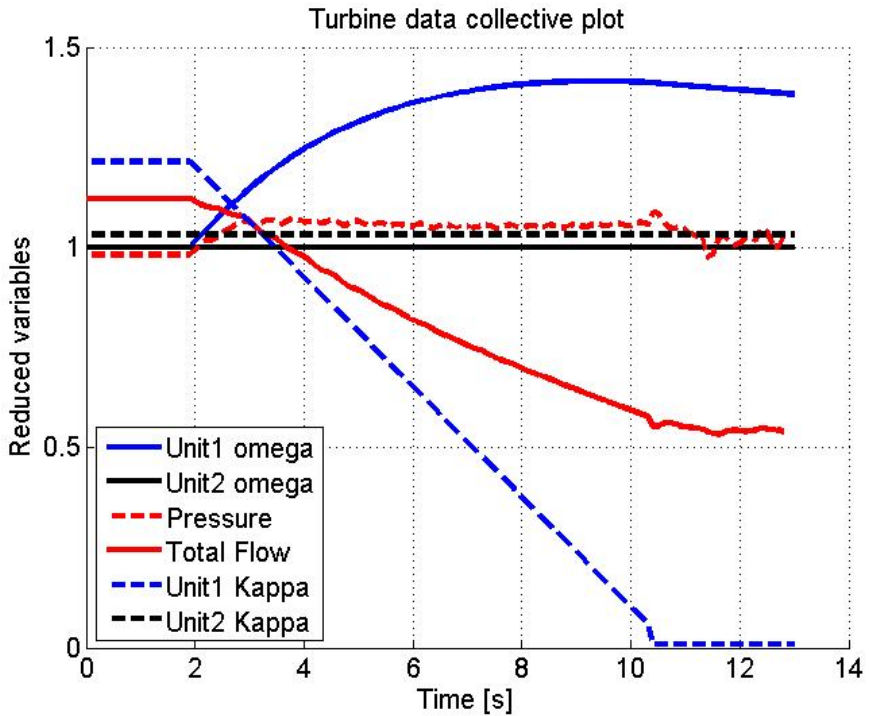


Figure 5.6: System response during rejection of unit one

The simulation overestimate both the runaway speed and pressure surge by 18.10% and 16.67%, respectively. Based on the previous rejection simulation of unit two, the pressure overshoot was a slight surprise. However, upon further investigation of the rejection measurements, it became clear that the bypass valve was active during these rejections (See Appendix F). This valve will reduce the water hammer experienced by the turbines. This valve is poorly documented, but it is assumed that it is located in the spiral casing of unit 1. The rejection trials for unit two make no mention of this valve, and it is therefore assumed to be inactive during the trials for unit two, hence the results in the previous section are still considered valid. The valve explains the overestimation for this rejection, but also complicate its verification. In its present state, the model is unable to account for this effect. A simple model for this valve is suggested in chapter 6, but not implemented.

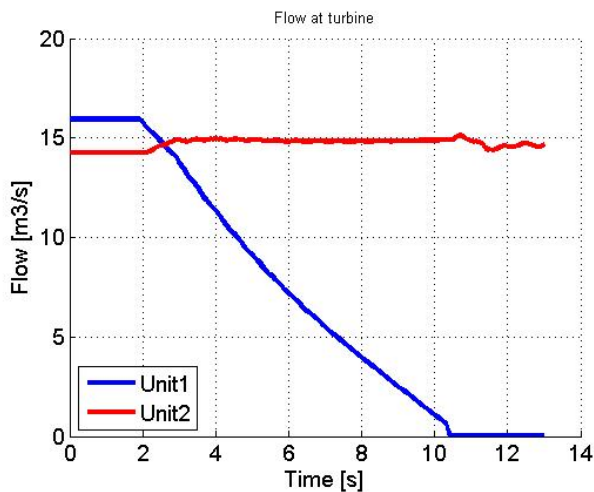


Figure 5.7: Flow transient during load rejection of unit one

Underestimation of tunnel frictional loss is also observed in this simulation. The possible reasons are assumed the same as in the previous section. As can be observed from figure 5.7, the increased pressure differential forces more water through the remaining unit.

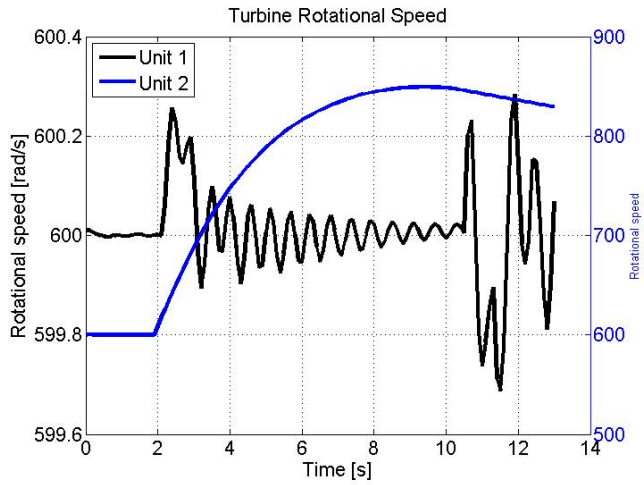


Figure 5.8: Rotational speeds during rejection of unit one

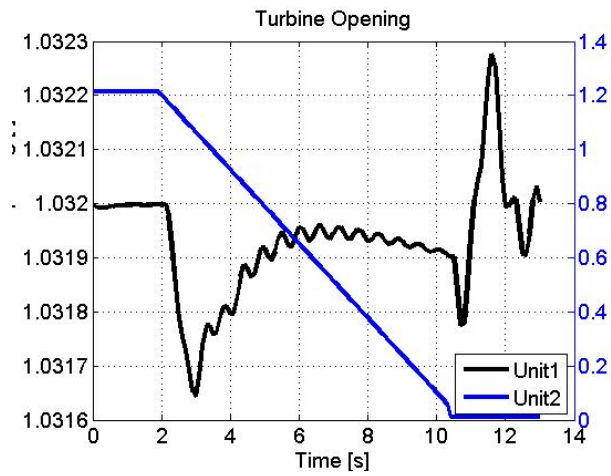


Figure 5.9: Guide vane position during rejection of unit one

The regulation of the unit that remains online (in this case unit two) is very similar to that observed in the previous section, and no new discrepancies are observed.

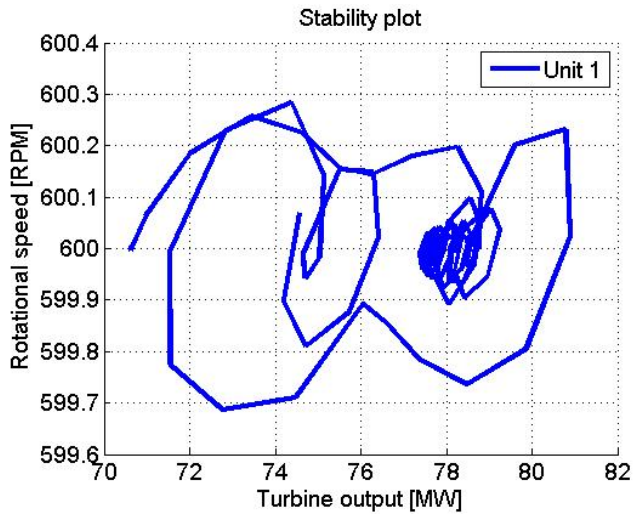


Figure 5.10: Shaft output of unit two during rejection of unit one

Unit one has a slower servo than unit two, and closes the guide vanes slower. The stabilization around a new output power can not be observed due to the simulation ending.

5.2 Immediate closure of both units

In order to further verify the solver for the waterway, it is of interest to compare the response to known analytical solutions. The turbine guide vanes were closed immediately while running on nominal load (total flow of $26.9 \frac{m^3}{s}$) over one time increment. The intent was to compare the surge magnitude to that given by Joukowski (2.3) and ideal oscillation periods.

Table 5.3: Results: Instant closure

Type	Simulated	Analytical	Difference
Pulsation period	1.2 seconds	1.2 seconds	0 %
Max pressure surge	1490	1487.82	0.14 %

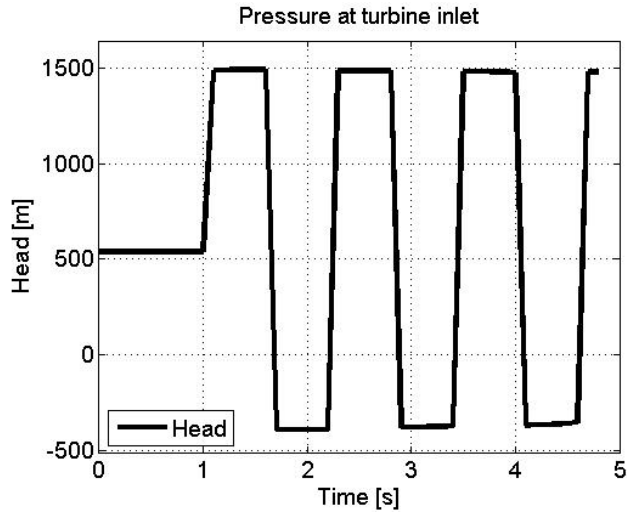


Figure 5.11: Pressure surge following an immediate closure

Under these theoretical circumstances, the simulation yields the analytical solution with excellent accuracy.

5.3 Load variations

The intention of the author was to implement a model that could visualize the impact of grid fluctuations on the waterway. This was tested by simulating load variations by altering the grid frequency.

5.3.1 Step variation

Grid frequency was immediately changed from 50 hz to 50.1 hz. After 20 seconds it was changed back to 50 Hz. The purpose of this was to observe the general response, as well as the influence of permanent speed droop. The speed droop setting was set equal for generator and turbine governor, and was 10 % and 90 % for unit one and unit two, respectively.

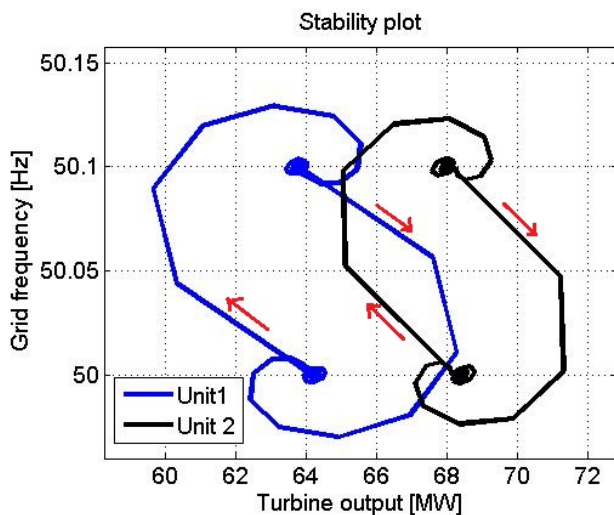


Figure 5.12: Load response following step changes in frequency

As can be observed from figure 5.12 the load response seems to be independent of speed droop setting, as both units regulate according to the same load distribution line. This is an indication that the regulators are not operating as intended. However, they do operate consistently, meaning upon regulation back to 50 Hz, the units regulate back to their initial operating point.

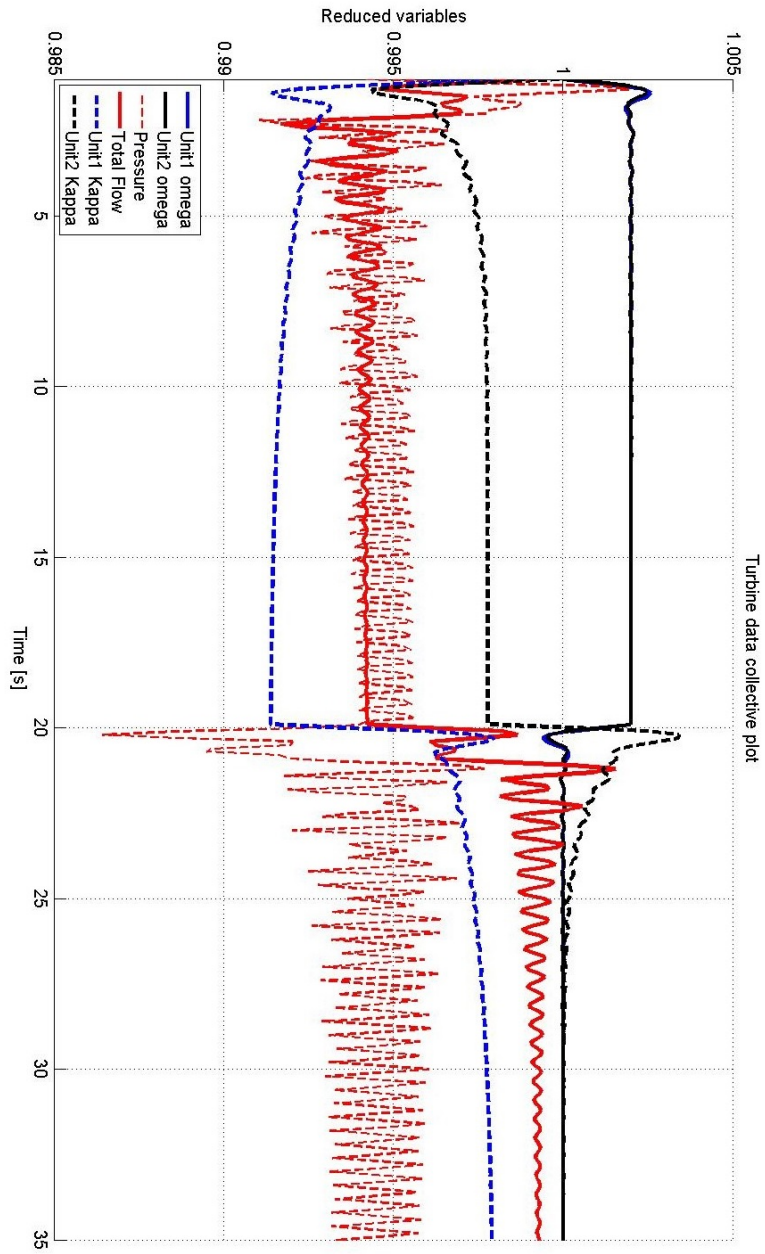


Figure 5.13: Plant response following step changes in frequency

Upon further observation of figure 5.13 it becomes clear that the magnitude of regulation upon a relatively large change in load is considerably less than expected. Both units close less than 1 %, and the change in output is much less than expected, resulting in very steep load distribution lines. This is not a realistic governor response. However, the magnitude of guide vane regulation does differ between the two units, indicating that the speed droop setting does indeed influence the governors. Just to a much less extent than planned. Two reasons for this might exist. The author may have incorrectly implemented the regulator functionality, or the equations might have flaws in their definition.

Other parts of the model seem to operate well, the dynamics being what one might expect from the change in turbine opening. Flow is reduced upon frequency increase, and increased upon frequency decrease, with a resulting pressure response. The turbine rotational speed quickly stabilize around the new steady state, with some fluctuations. These can be identified as variations in the magnetic displacement angle, which is shown in figure 5.14.

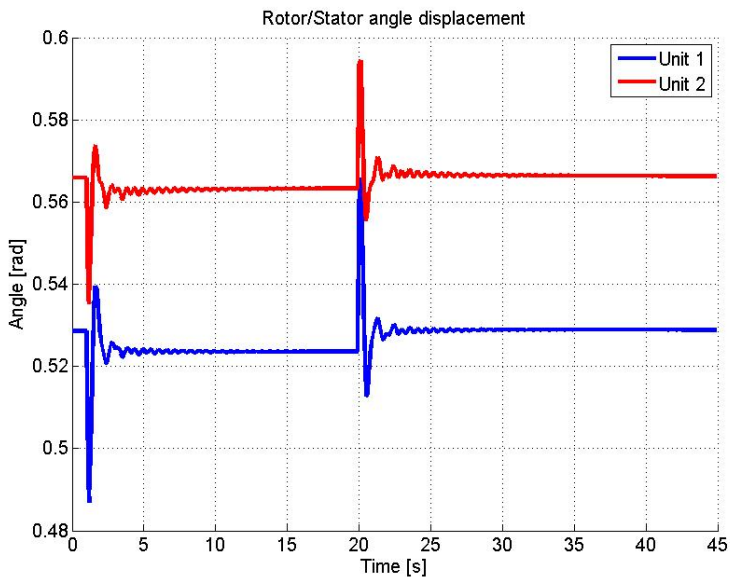


Figure 5.14: Magnetic displacement angle during step load changes

Step variations are also a suited scenario for observing surge chamber behaviour

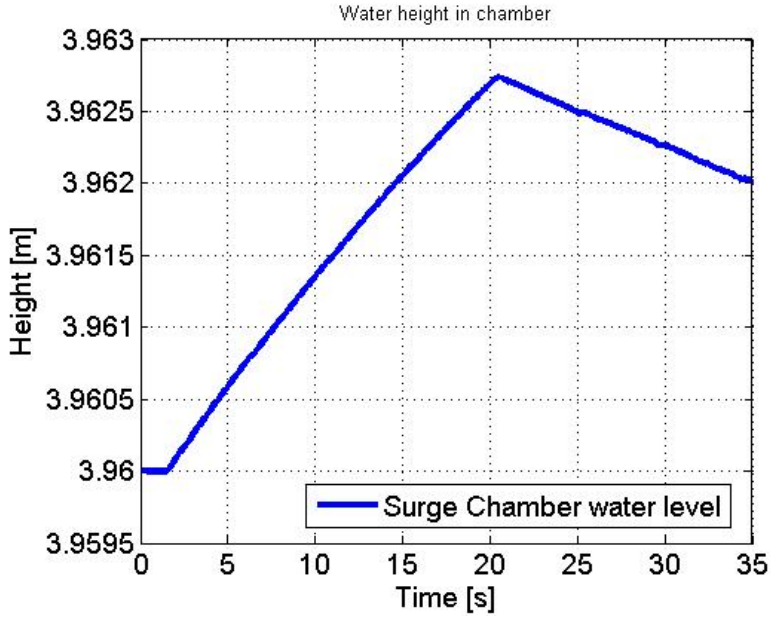


Figure 5.15: Surge chamber water level during step load changes

Upon a negative regulation, the deceleration of the water string causes water to flow into the surge chamber. Immediately upon the following positive regulation, the water starts to flow back out. Due to the small magnitude of regulation, the water level only rises slightly. However, the general behaviour is what should be expected from this system component.

5.3.2 0.6 % sine variation with period equal to oscillation period

The frequency was set to follow a sine function around 50 Hz with amplitude 0.3 Hz and period equal to pressure oscillation period between the turbines and the surge chamber. This was 1.2 seconds. The max amplitude of 50.3 Hz is high, this was to correct for the weak governor response observed during the previous simulation.

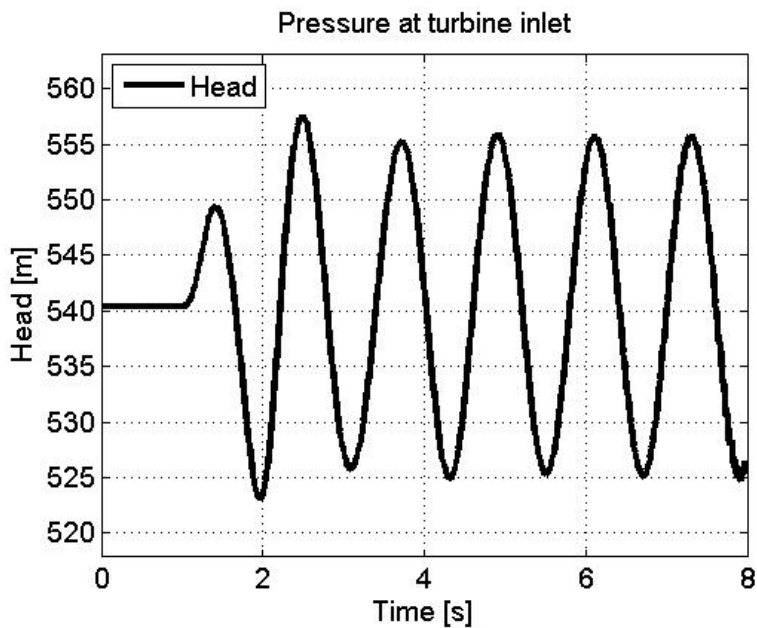


Figure 5.16: Periodic water hammer following sine regulation pattern

Table 5.4: Data for sine regulation

Max ΔQ	Joukowsky max surge	Simulated max surge	Difference
$0.4 \frac{m^3}{s}$	14.14 m	34.3 m	142.57 %

As can be observed from figure 5.16 and table 5.4, a small periodic change in

flow can induce large pressure variations. This is due to the pressure wave from the previous regulation period reflecting back just in time to amplify the magnitude of the current regulation period. This was expected and the ability to simulate these conditions provides a strong indication that the waterway model is suitable for analysing complex transient regulation patterns that may occur when the plant is actively trying to maintain grid stability.

Chapter 6

Conclusion and further work

The turbine model, coupled with using the method of characteristics for solving the waterway, show great promise regarding the initial predictions of dynamic behaviour of hydropower plants. This became clear when calibrating the model towards the Driva hydropower system, and subsequently simulating load rejections.

Some difficulties were encountered when trying to calibrate the turbine efficiency for conditions outside of optimum. The reason for the discrepancy was discovered, but not corrected due to lack of time. This should be corrected in any further work.

The generator model seems so be able to operate sufficiently, and seems to be a good initial model. This was based on its general behaviour only, as the author did not have measurement data for comparison.

Much difficulty was encountered both during the implementation and testing of the governor models. They were able to govern both generator and turbine models, but the amplitude of regulation upon a disturbance was less than expected, and the permanent speed droop settings was not sufficiently reflected in their behaviour. The author recommends further investigation into both the turbine and generator governor models.

The author also has the following recommendations for further work.

- Implement more editable properties into the GUI.
- Implement a better tunnel friction calculation scheme, as the model showed sign of miscalculating the head loss for other states than that for which it was calibrated.
- The numerical solver is suspected of being very inefficient. An alternative solver might be considered.
- Expand the waterway model to account for a non-constant speed of sound. See [15] for more information regarding modelling of the wave propagation speed.
- Modify loss modelling so that it accounts for viscous zero-flow spin losses in the turbine.
- Modelling of the bypass valve in unit one, this can be done by a simple valve with a pressure threshold before opening, see [15]. The flow through the valve can then be added to solution from the turbine/generator unit in order to observe the reduction in water hammer.
- A better power grid model should be implemented, one that has capacitance and more nodes.

List of Figures

1.1	Principal sketch of a hydropower system[8]	1
2.1	Pressure wave front propagating through a pipe	5
2.2	Collocated position-time grid where pressure and flow are computed in the same points.	7
2.3	Surge shaft and surge chamber [2]	8
2.4	Surgechamber model	9
2.5	Turbine suitability diagram[3]	11
2.6	Spiral casing with runner[3]	12
2.7	Francis inlet/outlet velocity diagram[3]	13
2.8	The sum of all losses creates the efficiency diagram[3].	15
2.9	Turbine with generator	18
2.10	Magnetic displacement angle between generator rotor and stator	19
2.11	Generator torque as a function of displacement angle	21
2.12	Power system illustration	22
2.13	Speed droop and power distribution line for two units creating their own grid	23
2.14	Turbine assembly with regulators[1]	25
3.1	Program overview	30
3.2	Simulation routine flowchart	31
3.3	Program overview	32
4.1	Input geometry for the simulation	36
4.2	Example of measurement of acceleration time constant	38
4.3	Declining rpm slope for calibration	39
5.1	System response during rejection of unit two	42

5.2	Pressure transient during load rejection of unit two	43
5.3	Rotational speeds during rejection of unit two	44
5.4	Guide vane position during rejection of unit two	44
5.5	Shaft output of unit one during rejection of unit two	45
5.6	System response during rejection of unit one	46
5.7	Flow transient during load rejection of unit one	47
5.8	Rotational speeds during rejection of unit one	48
5.9	Guide vane position during rejection of unit one	48
5.10	Shaft output of unit two during rejection of unit one	49
5.11	Pressure surge following an immediate closure	50
5.12	Load response following step changes in frequency	51
5.13	Plant response following step changes i frequency	52
5.14	Magnetic displacement angle during step load changes	53
5.15	Surge chamber water level during step load changes	54
5.16	Periodic water hammer following sine regulation pattern	55
D.1	Usage of C-characteristics in the t-x plane	90
D.2	Collocated position-time grid where pressure and flow are com- puted in the same points.	91

List of Tables

3.1	GUI input for turbine and generator	33
3.2	Output for simulated turbine/generator units	33
4.1	The general system has the following properties	35
4.2	The two installed units have the following properties at peak efficiency[6] [13]	36
4.3	Waterway division	37
4.4	Calibrated waterway frictional loss coefficients	37
4.5	Inertia and time constants	38
4.6	Calibrated turbine/generator frictional loss coefficients	39
4.7	Calibrated turbine viscous loss coefficients	40
4.8	Calibrated turbine angle loss coefficients	40
5.1	Simulated rejection data for unit two compared to measured data	42
5.2	Rejection data for unit one compared to measured data	46
5.3	Results: Instant closure	50
5.4	Data for sine regulation	55
C.1	Turbine input data during load rejections	88
C.2	Generator input data during load rejections	88
C.3	Turbine input data during load variations	88
C.4	Generator input data during load variations	88

Bibliography

- [1] Jens G. Balchen, Trond Andresen, and Bjarne A. Foss. *Reguleringsteknikk*. Institutt for Teknisk Kybernetikk, NTNU, 2004.
- [2] Hermod Brekke. *Regulering av Hydrauliske Strømningsmaskiner*. Vannkraftlaboratoriet NTNU, 2003.
- [3] Ole G. Dahlhaug. Turbomachinery lecture notes. TEP4195.
- [4] A.E. Fitzgerald, Charles Kingsley Jr, and Stephen D. Umans. *Electric Machinery*. McGraw-Hill, 1992.
- [5] Einar Kobro, Leif Parr, and Eivind Oppedal Olsen. Driva aggregat 2 avlagsmåling og servovindikering 2012-01-04. Technical report, Norconsult, 2012.
- [6] Einar Kobro, Leif Parr, and Eivind Oppedal Olsen. Driva kraftverk virkningsgradmåling turbin 2. Technical report, Norconsult, 2012.
- [7] Xinxin Li. Driva hydropower plant regulation stability analysis. Technical report, Norconsult, 2011.
- [8] Torbjørn Nielsen. *Dynamisk Dimensjonering av Vannkraftverk*. NTNU Vannkraftlaboratoriet, 1990.
- [9] Torbjørn Nielsen. *Transient Characteristics of High Head Francis Turbines*. PhD thesis, NTH, 1990.
- [10] Torbjørn Nielsen. *Analytic Model For Dynamic Simulations of Francis Turbines - Implemented in MOC*. -, 1992.
- [11] Torbjørn K. Nielsen and Finn O. Rasmussen. *Frekvensregulering ved store lastendringer*. SINTEF Strømningsmaskiner, 1994.

- [12] Erik Nilsen. Driva kraftverk turbin 1, del b, falltapsmåling av sjakt og tunnel. Technical report, SINTEF, 1991.
- [13] Erik Nilsen. Driva kraftverk virkningsgradmåling turbin 1. Technical report, Norconsult, 2010.
- [14] Leif Parr. Driva kraftverk aggregat 1 avlagsmåling og servindikering etter bytte av løpehjul. Technical report, Norconsult, 2010.
- [15] Benjamin E. Wylie and Victor L. Streeter. *Fluid Transients*. Feb Press, 1988.

Appendix A

Model source code

```

function [results] = DrivaSIM(datacarrier)
global unit1_data
global unit2_data
%% PRE PROCESSING
g = 9.81; %Gravity constant
a = datacarrier.wavespeed; %Speed of sound in fluid
%----- SIMULATION DATA -----
dt = datacarrier.dt; %Timestep
dx = dt*a; %Length increment
tmax = datacarrier.tmax; %Simulation time
%----- DATA RESERVOIR -----
Hres = datacarrier.Hr; %Reservoir reference head
Hout = 91; %Outlet reference head
Hr = Hres - Hout; %Turbine pressure without loss
%----- TUNNEL PROPERTIES -----
f = datacarrier.frictionfactor; %Friction factor tunnel
fpenstock = 0.0059*1.73; %Friction factor penstock
%----- DATA HEADRACE1 -----
A1 = 20; %Flow area tunnel
L1 = 15000; %Length tunnel
D1 = sqrt(4*A1/pi); %Diameter tunnel
N1 = L1/dx; %Number of sections
%----- DATA HEADRACE2 -----
A2 = 22; %Tunnel area
L2 = 5520; %+1dx due to valvesection OBS OBS OBS
D2 = sqrt(4*A2/pi); %Tunnel diameter
N2 = L2/dx; %Number of base tunnel elements
%----- DATA SURGE CHAMBER -----
surgeHeight = zeros(1,tmax/dt); %Initiate dataholder surge chamber
height
%----- DATA PENSTOCK -----
A3 = 3.46; %Tunnel area
L3 = 360;
D3 = sqrt(4*A3/pi); %Tunnel diameter
N3 = L3/dx;
%----- SETTING GRID POSITION INDICES -----
pipestart1 = 1; %Start coordinate pipe 1
pipeend1 = N1; %End coordinate pipe 1
pipestart2 = pipeend1 + 1; %Start coordinate pipe 2
pipeend2 = pipestart2 + N2; %End coordinate pipe 2
surgepos = pipeend2 + 1; %Coordinate of surge chamber
pipestart3 = surgepos + 1; %Start coordinate penstock
pipeend3 = pipestart3 + N3; %End coordinate penstock
valvepos = pipeend3 + 1; %Coordinate of valve/turbine
%----- INPUT CHECK -----
if dx/round(dx) ~= 1
    error('inconsistent CFL. Check a or dt')
end
if N1/round(N1) ~= 1
    error('length/section mismatch upstream. Check L1')
end
if N2/round(N2) ~= 1
    error(['length/section mismatch downstream ', num2str(N2/round(N2)), '.
', 'Check L2'])
end
R1 = f*dx/(2*g*(D1^5)*(pi/4)^2); %headloss per section of pipe (rock)

```

```

R2 = f*dx/(2*g*(D2^5)*(pi/4)^2);           %headloss per section of pipe (rock)
R3 = fpenstock*dx/(2*g*(D3^5)*(pi/4)^2);   %headloss per section of pipe
(penstock)
B1 = a/(g*A1);                             %MOC1 constant
B2 = a/(g*A2);                             %MOC2 constant
B3 = a/(g*A3);                             %MOC3 constant
%%%%%%%%%%%%%%%%%%%%%%%%%%%%%%%%%%%%%%%%%%%%%%%%%%%%%%%%%%%%%%%%%%%%%%%%
%% SIMULATION INITIATION
%%%%%%%%%%%%%%%%%%%%%%%%%%%%%%%%%%%%%%%%%%%%%%%%%%%%%%%%%%%%%%%%%%%%%%%%
data = zeros(2, valvepos, tmax/dt);         %initiation of return data holder
Qp = zeros(1, valvepos);                   %Qp (flow for current time)
Hp = zeros(1, valvepos);                   %Hp (head for current time)
Q = zeros(1, valvepos);                    %Q (flow for previous time increment)
H = zeros(1, valvepos);                    %H (head for previous time increment)

%%%%%%%%%%%%%%%%%%%%%%%%%%%%%%%%%%%%%%%%%%%%%%%%%%%%%%%%%%%%%%%%%%%%%%%%
%% DECLARING TURBINE UNITS
%%%%%%%%%%%%%%%%%%%%%%%%%%%%%%%%%%%%%%%%%%%%%%%%%%%%%%%%%%%%%%%%%%%%%%%%
%Declaring data unit 1
unit1_data.unitID = 1;                     %Turbine nr for
identification
unit1_data.turbinestatus = 'open';         %Status of
turbine(open/closed)
unit1_data.generatorstatus = 'online';     %Status of
generator(offline/online)
unit1_data.gen_delta = zeros(1, tmax/dt);  %Generator angular
displacement
unit1_data.gen_voltage = unit1_data.gen_delta; %Generator output
voltage
unit1_data.gen_current = unit1_data.gen_delta; %Generator output
current
unit1_data.gen_ko = unit1_data.gen_delta;  %Generator output
current
unit1_data.turb_omega = unit1_data.gen_delta; %Rotor angular speed
unit1_data.kappa = unit1_data.gen_delta;  %Guide vane opening
unit1_data.c = unit1_data.gen_delta;      %Servo speed
unit1_data.flow = unit1_data.gen_delta;   %Flow
unit1_data.power = unit1_data.gen_delta;  %Generator power w/o
loss
unit1_data.etah = unit1_data.gen_delta;   %Hydraulic efficiency
unit1_data.eta = unit1_data.gen_delta;    %Total efficiency

% Collecting data and placing in dataholder for simulation routine
unit1_data.Rm = datacarrier.Rm1;
unit1_data.Ra = 0.6;
unit1_data.Rf = 0.0205;
unit1_data.deltat = datacarrier.deltat1;
unit1_data.deltab = datacarrier.deltab1;
unit1_data.Ti = datacarrier.Ti1;
unit1_data.Pref = datacarrier.Pref1;
unit1_data.Pnom = 65.37*10^6;
unit1_data.Hr = datacarrier.Hr1;
unit1_data.Qr = 13.12;
unit1_data.J = 118667;
unit1_data.deltaref = datacarrier.deltaref1;
unit1_data.Eref = datacarrier.Eref1;
unit1_data.deltatg = datacarrier.deltatg1;

```

```

unit1_data.deltabg = datacarrier.deltabg1;
unit1_data.genTi = datacarrier.genTi1;
unit1_data.simdata.t1 = datacarrier.t1_1;
unit1_data.simdata.t2 = datacarrier.t1_2;
unit1_data.simdata.t3 = datacarrier.t1_3;
unit1_data.simdata.model = datacarrier.model_1;
unit1_data.simdata.mode2 = datacarrier.model_2;
unit1_data.simdata.mode3 = datacarrier.model_3;

%Declaring data unit 2
unit2_data.unitID = 2;
unit2_data.turbinestatus = 'open';
unit2_data.generatorstatus = 'online';
unit2_data.gen_delta = zeros(1,tmax/dt); %Generator angular
displacement
unit2_data.gen_voltage = unit2_data.gen_delta; %Generator output
voltage
unit2_data.gen_current = unit2_data.gen_delta; %Generator output
current
unit2_data.gen_ko = unit2_data.gen_delta; %Generator output
current
unit2_data.turb_omega = unit2_data.gen_delta; %Rotor angular speed
unit2_data.kappa = unit2_data.gen_delta; %Guide vane opening
unit2_data.c = unit2_data.gen_delta; %Servo motor speed
unit2_data.flow = unit2_data.gen_delta; %Flow
unit2_data.power = unit2_data.gen_delta;
unit2_data.etah = unit2_data.gen_delta; %Hydraulic efficiency
unit2_data.eta = unit2_data.gen_delta; %Total efficiency

unit2_data.Rm = datacarrier.Rm2;
unit2_data.Ra = 0.6;
unit2_data.Rf = 0.01135;
unit2_data.deltat = datacarrier.deltat2;
unit2_data.deltab = datacarrier.deltab2;
unit2_data.Ti = datacarrier.Ti2;
unit2_data.Pref = datacarrier.Pref2;
unit2_data.Pnom = 69.5*10^6;
unit2_data.Hr = datacarrier.Hr2;
unit2_data.Qr = 13.81;
unit2_data.J = 82070;
unit2_data.deltaref = datacarrier.deltaref2;
unit2_data.Eref = datacarrier.Eref2;
unit2_data.deltatg = datacarrier.deltatg2;
unit2_data.deltabg = datacarrier.deltabg2;
unit2_data.genTi = datacarrier.genTi2;
unit2_data.simdata.t1 = datacarrier.t2_1;
unit2_data.simdata.t2 = datacarrier.t2_2;
unit2_data.simdata.t3 = datacarrier.t2_3;
unit2_data.simdata.model = datacarrier.mode2_1;
unit2_data.simdata.mode2 = datacarrier.mode2_2;
unit2_data.simdata.mode3 = datacarrier.mode2_3;

% Finding initial flow and efficiency to yield required generator output
etagenerator = 0.982; %Generator efficiency NOTE: MAY BE SET
NUMERICALLY ELSEWHERE
P1 = 0;

```



```

P2 = 0;
dq = 0.001;
q1 = dq;
q2 = dq;
Ptarget1 = unit1_data.Pref*10^6/etagenerator;
Ptarget2 = unit2_data.Pref*10^6/etagenerator;
% NOTE: THE VARIABLES ABOVE SHOULD BE IMPORTED DIRECTLY VIA A FUNCTION.
% THESE ARE SET BY FUNCTION AggregateMOCgenericMK2
alpha1r = 0.0615;
beta1r = 0.9562;
psi = 0.3020;
ksi2 = 1.305;
mr = 1.307;
Hs = -13.05;
hold on
%%%%%%%%%%%%%%%%%%%%%%%%%%%%%%%%%%%%%%%%%%%%%%%%%%%%%%%%%%%%%%%%%%%%%%%%
x = 1;
while P1 <= Ptarget1 || P2 <= Ptarget2
    Q0 = q1*unit1_data.Qr + q2*unit2_data.Qr;
    for i = 1:pipeend1
        H(i) = Hr - (i-1)*R1*Q0*Q0;           %Head will drop due to resistance
        Q(i) = Q0;                           %Flow will remain the same
    end
    for i = pipestart2:pipeend2
        H(i) = H(i-1) - R2*Q0*Q0;           %Head will drop due to resistance
        Q(i) = Q0;                           %Flow will remain the same
    end
    H(surgepos) = H(surgepos-1);
    Q(surgepos) = Q(surgepos-1);
    for i = pipestart3:valvepos
        H(i) = H(i-1) - R3*Q0*Q0;           %Head will drop due to resistance
        Q(i) = Q0;                           %Flow will remain the same
    end
    end

    % Finding startup variables for current iteration
    qdimc1 = ((1 + cot(alpha1r)*tan(beta1r))/(1 +
cot(asin(q1*sin(alpha1r))*tan(beta1r)));
    ms1 = ((1+psi)/mr)*ksi2*(cos(asin(q1*sin(alpha1r))) +
tan(alpha1r)*sin(asin(q1*sin(alpha1r))));
    etah1 = (1-((unit1_data.Rf*q1^2 + unit1_data.Ra*(q1-
qdimc1)^2)/(H(end)/unit1_data.Hr)));
    eta1 = (q1*(ms1 - psi)*etah1 - unit1_data.Rm)/(q1*(H(end)/unit1_data.Hr));

    qdimc2 = ((1 + cot(alpha1r)*tan(beta1r))/(1 +
cot(asin(q2*sin(alpha1r))*tan(beta1r)));
    ms2 = ((1+psi)/mr)*ksi2*(cos(asin(q2*sin(alpha1r))) +
tan(alpha1r)*sin(asin(q2*sin(alpha1r))));
    etah2 = 1-((unit2_data.Rf*q2^2 + unit2_data.Ra*abs(q2-
qdimc2)^2)/(H(end)/unit2_data.Hr));
    eta2 = (q2*(ms2 - psi)*etah2 - unit2_data.Rm)/(q2*(H(end)/unit2_data.Hr));

    P1 = eta1*9846.38*H(end)*q1*unit1_data.Qr;
    P2 = eta2*9846.38*H(end)*q2*unit2_data.Qr;

    %If target power is not reached, increase flow
    if P1 < Ptarget1

```

```

        q1 = q1 + dq;
    end
    if P2 < Ptarget2
        q2 = q2 + dq;
    end
    end
    x=x+1;

end
% Find steady state for entire pipe, for computation of P-points
Q0 = q1*unit1_data.Qr + q2*unit2_data.Qr;
for i = 1:pipeend1
    H(i) = Hr - (i-1)*R1*Q0*Q0;           %Head will drop due to resistance
    Q(i) = Q0;                           %Flow will remain the same
end
for i = pipestart2:pipeend2
    H(i) = H(i-1) - R2*Q0*Q0;           %Head will drop due to resistance
    Q(i) = Q0;                           %Flow will remain the same
end
H(surgepos) = H(surgepos-1);           %Setting pressure in surgechamber
(same node as the next)
Q(surgepos) = Q(surgepos-1);
for i = pipestart3:valvepos
    H(i) = H(i-1) - R3*Q0*Q0;           %Head will drop due to resistance
    Q(i) = Q0;                           %Flow will remain the same
end

data(1,:,1) = H;                         %Steady state properties (t = 0)
data(2,:,1) = Q;                         %"

t = 0;                                   %setting time
k = 1;                                   %counter

tic
%% SOLVER
while t < tmax
    %Boundary conditions RESERVOIR
    Hp(1) = Hr;
    Qp(1) = Q(2) + (Hp(1) - H(2) - R1*Q(2)*abs(Q(2)))/B1;

    %Computation of interior points PIPE 1
    for j = 2:pipeend1-1
        Cp = H(j-1) + Q(j-1)*(B1 - R1*abs(Q(j-1))); %MOC method
        Cm = H(j+1) - Q(j+1)*(B1 - R1*abs(Q(j+1)));
        Hp(j) = 0.5*(Cp+Cm);
        Qp(j) = (Cp-Hp(j))/B1;
    end
    %Boundary conditions junction pipel/pipe2
    Cp = H(pipeend1-1) + Q(pipeend1-1)*(B1 - R1*abs(Q(pipeend1-1)));
    Cm = H(pipeend1+1) - Q(pipeend1+1)*(B2 - R2*abs(Q(pipeend1+1)));
    Qp(pipeend1) = (Cp - Cm)/(B1 + B2);
    Hp(pipeend1) = Cm + B2*Qp(pipeend1);

    %Computation of interior points PIPE 2
    for j = pipestart2:pipeend2-1
        Cp = H(j-1) + Q(j-1)*(B2 - R2*abs(Q(j-1)));
        Cm = H(j+1) - Q(j+1)*(B2 - R2*abs(Q(j+1)));

```

```

        Hp(j) = 0.5*(Cp+Cm);
        Qp(j) = (Cp-Hp(j))/B2;
    end
    %Boundary conditions junction pipe2/pipe3
    Cp = H(pipeend2-1) + Q(pipeend1-1)*(B2 - R2*abs(Q(pipeend1-1)));
    Cm = H(pipeend2+2) - Q(pipeend1+2)*(B3 - R3*abs(Q(pipeend1+2)));
    Qp(pipeend2) = (Cp - Cm)/(B2 + B3);
    Hp(pipeend2) = Cm + B3*Qp(pipeend2);

    %Surge chamber
    [Hp,Qp,surgeHeight] =
    Surge_Chamber(Q,H,Qp,Hp,surgepos,B2,B3,R2,R3,dt,surgeHeight,k);

    %Computation of interior points PIPE 3
    for j = pipestart3:pipeend3
        Cp = H(j-1) + Q(j-1)*(B3 - R3*abs(Q(j-1)));
        Cm = H(j+1) - Q(j+1)*(B3 - R3*abs(Q(j+1)));
        Hp(j) = 0.5*(Cp+Cm);
        Qp(j) = (Cp-Hp(j))/B3;
    end

    %Boundary conditions VALVE/Turbine
    [unit1_data] = AggregateMOCgenericMK2(t,H,B3,R3,unit1_data,k,dt,q1);
    [unit2_data] = AggregateMOCgenericMK2(t,H,B3,R3,unit2_data,k,dt,q2);
    %FOR ADDING MORE UNITS, DECLARE HERE AS WELL AS 1 MORE BLOCK OF
    %TURBINE DECLARATION ABOVE

    Cp = H(end-1) + Q(end-1)*(B3 - R3*abs(Q(end-1)));
    Qp(end) = unit1_data.flow(k) + unit2_data.flow(k);           %Flow in inlets
    are sum of both units
    Hp(end) = Cp - B3*Qp(end);                                   %Calculating
    pressure

    %Data processing and preparation for next time iteration
    H = Hp;
    Q = Qp;
    data(1,:,k) = Hp;                                           %Inserting fresh data into dataholder
    data(2,:,k) = Qp;                                           %"

    t = t + dt;                                                 %Updating time counter
    k = k + 1;                                                   %Updating time vector position counter

    %Updating GUI
    percentage = floor(t/tmax*100);
    set(objectfinder('simstatus_percentage'),'string',[num2str(percentage),'
%' ] )
    drawnow expose
end
%Creating resultsvector for return to GUI
results.H = data(1,:,:) ;
results.Q = data(2,:,:) ;
results.tmax = tmax;
results.dt = dt;
results.surgepos = surgepos;
results.turbinepos = valvepos;
results.surgeHeight = surgeHeight;

```

```
results.unit1_data = unit1_data;  
results.unit2_data = unit2_data;  
end
```

```

function [Hp,Qp,surgeheight] =
Surge_Chamber(Q,H,surgepos,B,R,Vgas,z,dt,C,mode,n,Hchamber,k)

global C
global Vgas
global z
mode = 'enable';
%Chamber dimensions
SurgeD = 10;
SurgeH = 10;
SurgeL = 77.5;
%Chamber polytropic exponent
n = 1.2;
Vsurge = SurgeD*SurgeH*SurgeL;
Vgas0 = 4681; %Initial gas volume
Vfluid = Vsurge - Vgas0; %Volume of fluid
z0 = Vfluid/(SurgeL*SurgeD); %Starting water level

if isempty(C)
    Hjunction0 = H(surgepos);
    C = (Hjunction0 - z0)*(Vgas0)^n; %Calculation of chamber constant
    Vgas = Vgas0;
    z = z0;
end

%Junction data
A3 = 12;
D3 = sqrt((4*A3)/pi);
f3 = 0.05;
L3 = 10;

if strcmp(mode,'enable')

    %From previous timestep
    Cp = H(surgepos-2) + Q(surgepos-2)*(B2 - R2*abs(Q(surgepos-2)));
    Cm = H(surgepos+1) - Q(surgepos+1)*(B3 - R3*abs(Q(surgepos+1)));
    Q1 = Q(surgepos - 1);
    Q2 = Q(surgepos + 1);
    H4 = Hchamber - z;
    C2 = ((2*L3)/(g*A3*dt));
    C1 = H4 - H + ((f3*L3)/(g*D3*A3))*Q3*abs(Q3) - C2*Q3;

    %symbolic variable for the solver
    syms Hp
    syms Hp4
    syms Qp1
    syms Qp2
    syms Qp3
    syms znew

    %Equations to be solved
    EQ1 = C1 + C2*Qp3 + L3 - Hp + Hp4;
    EQ2 = (Hp4 + zint)*(Vgas - (0.5*dt*(Qp3 + Q3)))^n - C;
    EQ3 = Qp1 - Qp3 - Qp2;
    EQ4 = Cp - B*Qp1 - Hp;
    EQ5 = Cm + B*Qp1 - Hp;

```

```

EQ6 = SurgeH - ((Vgas - 0.5*dt*(Qp3 + (Q1 - Q2)))/(SurgeD*SurgeL)) - zint;

solutions = newton_n_dim(0.1,[H H4 Q1 Q2 Q3 z],[Hp Hp4 Qp1 Qp2 Qp3
zint],[EQ1;EQ2;EQ3;EQ4;EQ5;EQ6]);
solutions = double(solutions);

%Setting the new variables into dataholders
Hp(surgepos) = solutions(1);
Qp(surgepos) = nsolutions(4);
chamberflow = nsolutions(5);

Vgas = Vgas - 0.5*dt*(chamberflow + (Q1 - Q2));
surgeheight(k) = SurgeH - (Vgas/(SurgeD*SurgeL));
z = surgeheight(k);

elseif strcmp(mode,'disable') %For disabling the chamber
Cp = H(surgepos-1) + Q(surgepos-1)*(B - R*abs(Q(surgepos-1)));
Cm = H(surgepos+1) - Q(surgepos+1)*(B - R*abs(Q(surgepos+1)));
Hpipe = 0.5*(Cp+Cm);
Qout = (Cp-Hpipe)/B;
Qin = NaN;
Vgas = NaN;
z = NaN;
end
end

```

```

function [unit_data] = AggregateMOCgenericMK2(t,H,B,R,unit_data,k,dt,qinitial)

%% Fluid properties
g = 9.81; %gravity acceleration constant
%% TURBINE PROPERTIES
Qr = unit_data.Qr; %Rated flow at design point per turbine
nref = 600;
omegar = nref*2*pi/60;
%% CREATION OF BASE EULER TURBINE
U2r = 40;
turbacc = 1.1;
%reac = 0.5;
%eta = 0.96;
Hred = sqrt(2*g*unit_data.Hr);
% Clu = sqrt(eta - reac)*Hred;
% U1r = eta/(2*Clu/Hred)*Hred;
% r1 = U1r/(omegar);
% r2 = (U2r)/omegar;
% sigmageo = (2*r1)^2/8*(1-(r2/r1)^2)*2*(omegar/Hred)^2;
% r2 = sqrt((2*r1)^2-4*(sigmageo)/(2*(omegar/Hred)^2))/2;
% C2m = Qr/(pi*(r2^2));
% Clm = C2m/turbacc;
% b = Qr/(Clm*2*pi*r1);
% alphalr = atan(Clm/Clu);
% beta2 = atan(C2m/U2r);
% V2 = (C2m/Hred)/sin(beta2)*Hred;
% Clr = (Clm/Hred)/sin(alphalr)*Hred;
% betalr = atan(Clm/(Clr-Clu));
% sigmaeuler = (1 - (2*(U2r/Hred)^2))/(1 + (2*(U2r/Hred)^2));
% DATA BELOW SET FROM EXTERNAL EXCEL SHEET. EQUIVALENT TO COMPUTATIONS
% ABOVE
Clu = 0.678233*Hred;
U1r = 0.7077*Hred;
r1 = 2.31877/2;
r2 = 1.2732/2;
sigmageo = 0.3498;
C2m = Qr/(pi*(r2^2));
Clm = C2m/turbacc;
b = Qr/(Clm*2*pi*r1);
alphalr = 0.0615;
beta2 = 0.1177;
Clr = 0.6795*Hred;
betalr = 0.9562;

%% STEADY STATE INITIATION OF VARIABLES
%Loss variables
Rm = unit_data.Rm;
Ra = unit_data.Ra;
Rf = unit_data.Rf;
%Generator variables
omegagrid = 2*pi*50; %Reference grid omega
P = 2*(omegagrid/omegar); %Generator poles
Pratedgen = unit_data.Pref*10^6; %Rated power generator (USER SET)
Tratedgen = Pratedgen/omegagrid; %Generator magnetic torque (Geared by P/2)
qdimcr = 1*((1 + cot(alphalr)*tan(betalr))/(1 + cot(alphalr)*tan(betalr)));

```

```

hydraulicloss0 = (1-((Rf*qinitial^2 + Ra*(qinitial-
qdimcr)^2)/(H(end)/unit_data.Hr)));
Prated = Pratedgen/((hydraulicloss0 - Rm)*qinitial); %Rated power turbine
Trated = Prated/omegar; %Rated torque turbine
Urated = unit_data.Eref; %Rated voltage generator (USER SET)
korated = Urated/((P/2)*omegar); %Rated magnetic constant
Irated = Tratedgen/korated; %Rated voltage generator

PgenMAX = 90*10^6; %Generator maximum output
TgenMAX = PgenMAX/omegagrid; %Generator maximum torque
deltaMAX = pi/4; %Displacement angle at maximum output
deltaref = asin((Tratedgen/TgenMAX)*sin(deltaMAX));

Rgridref = Urated/Irated;
Rgrid = Rgridref;
%% REGULATION CONSTANTS
Uregref = Urated; %Set reference voltage for governor
Iregref = Irated; %Set reference current for governor
kapparegref = 1; %Set reference kappa for governor
%% EQUATION CONSTANTS AND SIMPLIFICATIONS
psi = U2r^2/(g*unit_data.Hr); %Turbine pressure number
ksi2 = (psi + 1)/(cos(alphalr)); %Turbine dimensionless machine constant
%Jpolar = mrotor*(0.735*r1); %Rotor polar moment of inertia
Jpolar = unit_data.J;
Ta = Jpolar*(omegar^2/unit_data.Pnom); %Rotor time constant

sigmaloss = -(1 - psi*(1 - Rf) - 2*Rm)/(2*Rf*((1+Rm)/(1-Rf)) - psi*(1 - Rf) -
1-2*Rm);

%Statics
deltat = unit_data.deltat; %Transient speed droop turbine (Kp
= 1/deltat). Lower is faster
Td = unit_data.Ti; %Integration time
deltab = unit_data.deltab; %Permanent speed droop turbine
Tk = 0.000001; %Servo time constant (set to
instant reaction)
deltatg = unit_data.deltatg; %Transient speed droop generator
Tdg = unit_data.genTi; %Integration time generator
deltabg = unit_data.deltabg; %Permanent speed droop generator
md = 0.02; %Magnetic damping constant

K1 = 1/(deltat*nref); %turbine constant1
K2 = 1/(deltat*Td); %turbine constant2
K3 = (deltab*Tk + deltat*Td)/(deltat*Td); %turbine constant3
K4 = deltab/(deltat*Td); %turbine constant4
K5 = 1/(deltatg*Uregref); %generator constant1
K6 = 1/(deltatg*Tdg*Uregref); %generator constant2
K7 = 1/(deltabg*Iregref); %generator constant3
%% EXTRACTING VALUES FOR PREVIOUS TIMESTEP AND SETTING STEADY-STATE VALUES
if t == 0 %If condition is initiation
    Uprev = Urated;
    omegadimprev = 1;
    kappaprev = qinitial;
    koprev = korated;
    cprev = 0;
    deltaprev = deltaref;

```



```

unit_data.flow(1) = qinitial*Qr;
qdimprev = qinitial;
Iprev = Irated;
Tgprev = Tratedgen*(P/2);

else
    Uprev = unit_data.gen_voltage(k-1);
    omegadimprev = unit_data.turb_omega(k-1)/omegar;
    kappaprev = unit_data.kappa(k-1);
    koprev = unit_data.gen_ko(k-1);
    cprev = unit_data.c(k-1);
    deltaprev = unit_data.gen_delta(k-1);
    qdimprev = unit_data.flow(k-1)/Qr;
    Iprev = unit_data.gen_current(k-1);
    Tgprev = ((sin(deltaprev)/sin(deltaref))*Tratedgen*(P/2));
end
%% SETTING SIMULATION SCHEDULE
eventtime1 = unit_data.simdata.t1;
eventtime2 = unit_data.simdata.t2;
eventtype1 = unit_data.simdata.model;
eventtype2 = unit_data.simdata.mode2;
residualevent = unit_data.simdata.mode3;

if unit_data.unitID == 1
    gridfactor1 = 1;
    gridfactor2 = 1;
    residualgridfactor = 1;
elseif unit_data.unitID == 2
    gridfactor1 = 1;
    gridfactor2 = 1;
    residualgridfactor = 1;
end

%CHANGES IN CONDITIONS MUST BE PUT IN BLOCKS BELOW
omegaregref = omegar;
if t <= eventtime1
    scheme = eventtype1;
    Rgrid = gridfactor1*Rgridref;
elseif t > eventtime1 && t <= eventtime2
    scheme = eventtype2;
    Rgrid = gridfactor2*Rgridref;
    omegagrid = 2*pi*50.2;
    %omegagrid = 2*pi*(50 + 0.3*sin(2*pi*((t-eventtime1 - dt)/1.2)))
    %omegaregref = omegaprev;
    % if t >= eventtime1 + 1
    %     qinitial = 1.1
    % end
    global omegagridprev;
    global omegagridholder
    % if omegagrid < omegagridprev
    %     omegagrid = omegagridprev;
    % end
    omegagridholder = omegagrid;
    omegagridholder(k) = omegagrid; %Saving frequency history
elseif t > eventtime2
    scheme = residualevent;

```

```

Rgrid = residualgridfactor*Rgridref;
omegagrid = 2*pi*49.7;
omegagrid = 2*pi*(50 + 0.1*sin(100*(eventtime2-eventtime1 - dt)));
end
%% DECLARATION OF SYMBOLIC VARIABLES FOR SOLVER
syms kappa
syms qdim
syms omegadim
syms ko
syms I
syms U
syms c
syms delta
syms Tg
%% TIME-STEP SPECIFIC VALUES
if t < 0.05
    Cp = H(end-1) + Qr*qinitial*(B - R*abs(Qr*qinitial));
else
    Cp = H(end-1) + unit_data.flow(k-1)*(B - R*abs(unit_data.flow(k-1)));
end
if ~isfield(unit_data, 'Hs')
    unit_data.Hs = Cp - B*Qr*qinitial - unit_data.Hr;
end
mr = ksi2*1*(cos(alphalr) + tan(alphalr)*sin(alphalr));
alphal = (asin(kappa*sin(alphalr)));
ms = ((1+psi)/mr)*ksi2*(abs(qdim)/kappa)*(cos(alphal) +
tan(alphalr)*sin(alphal));
%qdimc = ((Ain)*r1*tan(betalr))/(1 + cot(alphal)*tan(betalr));
qdimc = omegadim*((1 + cot(alphalr)*tan(betalr))/(1 +
cot(alphal)*tan(betalr)));

%% ----- ONLINE DYNAMIC REGULATION -----
if strcmp(scheme, 'Regulation')

    % DIFFERENTIAL EQUATIONS
    %Waterway equation
    EQ1 = Cp - B*Qr*qdim - unit_data.Hs -
unit_data.Hr*(1/(1+sigaloss))*((qdim/kappa)^2 + sigaloss*(omegadim^2));
    %Turbine torque equation
    EQ2 = qdim*(ms - psi*omegadim)*(1-((Rf*qdim^2 + Ra*abs((qdim-
qdimc))^2)/(H(end)/unit_data.Hr)) - Tg/Trated - Rm*omegadim^2 - md*((delta-
deltaprev)/dt) - (Ta/dt)*(omegadim - omegadimprev);
    %Generator angle equation in island mode
    %EQ3 = dt*((P/2)*omegadim*omegar - U/ko) - (delta - deltaprev);
    %Generator angle equation in static mode
    EQ3 = dt*((P/2)*omegadim*omegar - omegagrid) - (delta - deltaprev);
    % Kappa regulator equation
    EQ4 = dt*(qinitial/Tk)*(-K1*((omegadim*omegar -
omegadimprev*omegar)/dt)*(30/pi) + K2*((omegaregref -
omegadim*omegar)/omegaregref) - K3*c - K4*(qinitial - kappa)) - (c - cprev);
    %Voltage regulator equation
    EQ5 = -dt*(-K5*((U - Uprev)/dt) + K6*(Uregref + K7*(I - Iregrid) - U)) -
(ko - koprev);
    %Integration of kappa
    EQ6 = kappaprev + dt*c - kappa;
    % ALGEBRAIC EQUATIONS
    %Grid ohms law

```

```

EQ7 = Rgrid*((2*Tg)/(ko*P)) - U;
%Generator torque vs output equation
EQ9 = ((sin(delta)/sin(deltaMAX))*TgenMAX*(P/2)) - Tg;
%Generator torque equation
EQ8 = ko*I*(P/2) - Tg;

%Solving equation
nsolution =
newton_n_dim(0.1,[qdimprev,kappaprev,omegadimprev,cprev,deltaprev,Uprev,koprev
,Tgprev,Iprev],[qdim,kappa,omegadim,c,delta,U,ko,Tg,I],[EQ1;EQ2;EQ3;EQ4;EQ5;EQ
6;EQ7;EQ8;EQ9]);

solution(1) = double(nsolution(1));
solution(2) = double(nsolution(2));
solution(3) = double(nsolution(3));
solution(4) = double(nsolution(4));
solution(5) = double(nsolution(5));
solution(6) = double(nsolution(6));
solution(7) = double(nsolution(7));
solution(8) = double(nsolution(8));
solution(9) = double(nsolution(9));

unit_data.flow(k) = solution(1)*Qr;
unit_data.turb_omega(k) = solution(3)*omegar;
unit_data.c(k) = solution(4);
unit_data.kappa(k) = solution(2);
unit_data.gen_ko(k) = solution(7);
unit_data.gen_delta(k) = solution(5);
unit_data.gen_voltage(k) = solution(6);
unit_data.gen_current(k) = solution(9);
unit_data.omegaref = omegar;
unit_data.power(k) = solution(8)*solution(3)*omegar;

%qdimc = ((Ain/Aout)*r1*tan(beta1r))/(1 +
cot((asin(nsolution(2)*sin(alpha1r))))*tan(beta1r));
alpha = (asin(solution(2)*sin(alpha1r)));
qdimc = solution(3)*((1 + cot(alpha1r)*tan(beta1r))/(1 +
cot(alpha1)*tan(beta1r)));
ms = ((1+psi)/mr)*ksi2*(abs(solution(1))/solution(2))*(cos(alpha) +
tan(alpha1r)*sin(alpha1r));
unit_data.eta(k) = (1-((Rf*solution(1)^2 + Ra*(solution(1)-
qdimc)^2)/(H(end)/unit_data.Hr)));
unit_data.eta(k) = (solution(1)*(ms - psi*solution(3))*unit_data.eta(k) -
Rm*solution(3)^2)/(solution(1)*(H(end)/unit_data.Hr));

%% REJECTION
elseif strcmp(scheme,'Rejection')

unit_data.generatorstatus = 'offline';
if strcmp(unit_data.turbinesstatus,'open'); %IF TURBINE GUIDE VANES ARE
OPEN
    %maxclosuretime = 5.2;
    maxclosuretime = 7.28;

```

```

dkappa = dt/maxclosuretime;
kappa = kappaprev - dkappa;

alpha = (asin(kappa*sin(alpha_r)));
ms = ((1+psi)/mr)*ksi2*(abs(qdim)/kappa)*(cos(alpha) +
tan(alpha_r)*sin(alpha));
EQ1 = Cp - B*Qr*qdim - unit_data.Hs -
unit_data.Hr*(1/(1+sigmaloss))*((qdim/kappa)^2 + sigmaloss*(omegadim^2));
EQ2 = qdim*(ms - psi*omegadim)*0.92 - Rm*omegadim^2 -
(Ta/dt)*(omegadim - omegadimprev);

nsolution =
newton_n_dim(0.01,[qdimprev,omegadimprev],[qdim,omegadim],[EQ1;EQ2]);
nsolution = double(nsolution);
unit_data.flow(k) = nsolution(1)*Qr;
unit_data.turb_omega(k) = nsolution(2)*omegar;
unit_data.c(k) = kappa-kappaprev;
unit_data.kappa(k) = kappa;
unit_data.gen_ko(k) = 0;
unit_data.gen_delta(k) = 0;
unit_data.gen_voltage(k) = 0;
unit_data.gen_current(k) = 0;
unit_data.omegaref = omegar;

elseif strcmp(unit_data.turbinestatus,'closed') %IF TURBINE GUIDE VANES
ARE CLOSED
EQ2 = - (Ta/dt)*(omegadim - omegadimprev) - Rm*omegadim^2;
solution = solve(EQ2);
solution= max(double(solution));

unit_data.flow(k) = 0.01;
unit_data.turb_omega(k) = double(solution)*omegar;
unit_data.c(k) = 0;
unit_data.kappa(k) = 0.01;
unit_data.gen_ko(k) = 0;
unit_data.gen_delta(k) = 0;
unit_data.gen_voltage(k) = 0;
unit_data.gen_current(k) = 0;
unit_data.omegaref = omegar;
alpha = 0;

end
%IF unit is almost closed, set flow to small value to avoid division by
%zero.
if (unit_data.flow(k)/Qr) < 0.05
unit_data.turbinestatus = 'closed';
end
end
% DEBUG OUTPUT
disp('%%%%%%%%%%%%%%%%%%%%%%%%%%%%%%%%%%%%%%%%%%%%%%%%%%%%%%%%%%%%%%%%%%%%%%%%')
disp(['Unit nr: ',num2str(unit_data.unitID)])
disp(['Time is: ',num2str(t)])
disp(['Scheme is: ',scheme])
disp(['Kappa is: ',num2str(unit_data.kappa(k))])
disp(['C is: ',num2str(unit_data.kappa(k)-kappaprev)])

```

```
disp(['dC/dT is: ',num2str(unit_data.c(k)-cprev)])
disp(['Status is: ',unit_data.turbinestatus])
end
```


Appendix B

GUI Screenshot

- Simulation
- Conduits
- Turbine
- Generator**
- Events
- Results
- Settings

09-Jun-2013 13:56:39 Simulation completed (768.2351 seconds)
 09-Jun-2013 13:43:50 Simulation started
 09-Jun-2013 13:42:42 Oppstart

Generator properties

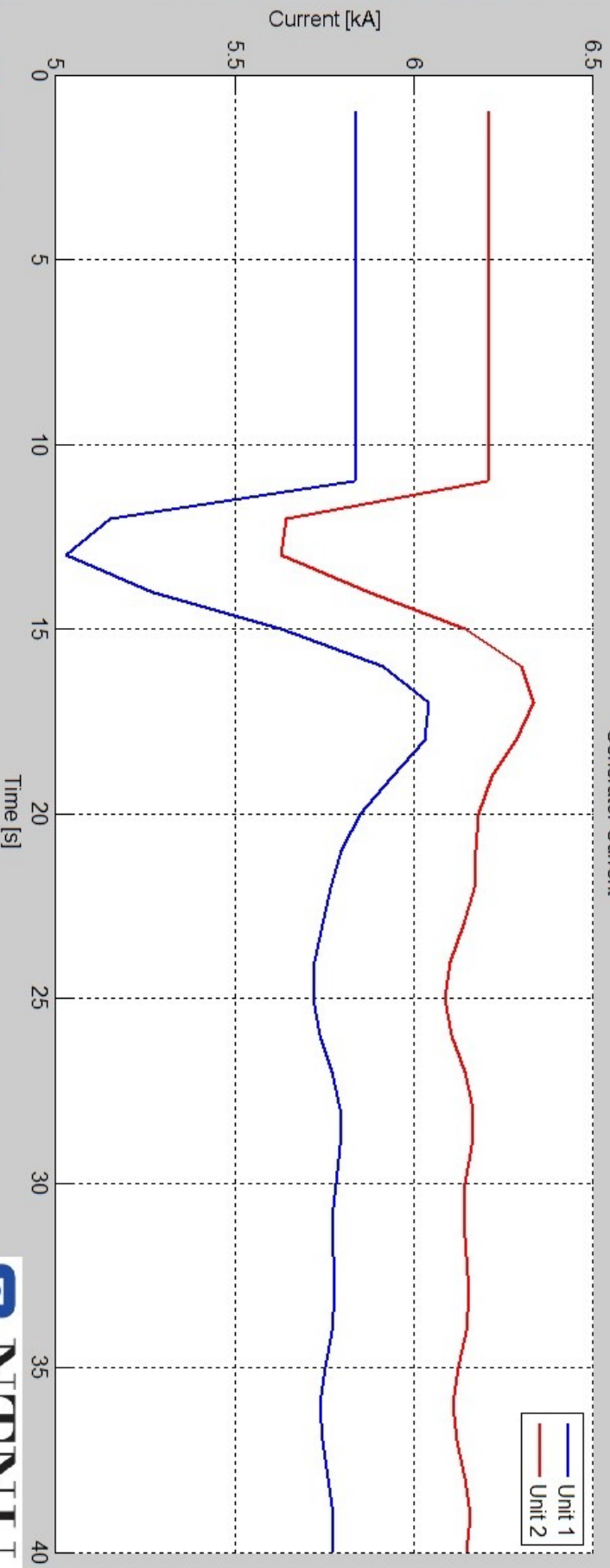
Generator 1

Output Power:	64.193
Ref delta:	pi
Rated voltage:	11000
Transient sd:	0.6
Permanent sd:	-0.05
Integration time:	6

Generator 2

Output Power:	68.249
Ref delta:	pi
Rated voltage:	11000
Transient sd:	0.6
Permanent sd:	-0.9
Integration time:	6

Generator Current



Complete 100 %

Appendix C

Simulation parameters for performed simulations

All calibrated values are as given in chapter 4.

Table C.1: Turbine input data during load rejections

Parameter	Turbine one	Turbine two
Transient sd	0.6	0.5
Permanent sd	-0.05	-0.05
Integration time	8	8
Rated head	540	540

Table C.2: Generator input data during load rejections

Parameter	Turbine one	Turbine two
Transient sd	0.6	0.6
Permanent sd	-0.05	-0.05
Integration time	6	6

Table C.3: Turbine input data during load variations

Parameter	Turbine one	Turbine two
Transient sd	0.4	0.4
Permanent sd	-0.1	-0.9
Integration time	4	4
Rated head	540	540

Table C.4: Generator input data during load variations

Parameter	Turbine one	Turbine two
Transient sd	0.4	0.4
Permanent sd	-0.1	-0.9
Integration time	4	4

Appendix D

Method of Characteristics

Introducing the multiplier λ , the following combination must be valid

$$L = L_1 + \lambda L_2 = gH_x + V_t + \frac{f}{2D}V|V| + \lambda(H_t + \frac{a^2}{g}V_x) = 0 \quad (\text{D.1})$$

(2.1) and (2.2) are now linearly combined, and any real distinct values of λ will result in two new equations. Choosing an appropriate value for λ , and manipulating yields

$$\frac{g}{a} \frac{dH}{dt} + \frac{dV}{dt} + \frac{fV|V|}{2D} = 0 \quad (\text{D.2})$$

for $\frac{dx}{dt} = +a$

$$-\frac{g}{a} \frac{dH}{dt} + \frac{dV}{dt} + \frac{fV|V|}{2D} = 0 \quad (\text{D.3})$$

for $\frac{dx}{dt} = -a$

The equations (2.1) and (2.2) have now effectively been separated into two cases, one for which the pressure wave is travelling in the opposite of the flow direction, and one for which the wave is propagating in the same direction as the flow. These two equations will be used to "bridge" data from one time increment to the next. (Complete manipulation can be found in Appendix A)

D.1 Finite difference discretization

In order to make equations (D.2) and (D.3) suitable for analysis, they need to be discretized to be valid for a conduit divided into a variable number of subsections, and be able to be solved along the given C characteristic to yield results for the next increment of time.

Manipulation of (D.3) by multiplying by $a \frac{dt}{g} = \frac{dx}{g}$ and rewriting the speed terms into volume flow terms, and then integrating along the characteristic line yield

$$\int_A^P dH + \frac{a}{gA} \int_A^P dQ + \frac{f}{2gDA^2} \int_A^P Q|Q|dx = 0 \quad (D.4)$$

Note that a first order approximation is used for the unknown flow under the integral in the last term. The same procedure is executed for the C- characteristic, and thus yielding two discrete equations for the already known values Q_A and Q_B from the previous time increment, and the unknown values Q_P and Q_P for the current time increment.

$$C+ : H_P = H_A - B(Q_P - Q_A) - RQ_A|Q_A| \quad (D.5)$$

$$C- : H_P = H_B + B(Q_P - Q_B) + RQ_A|Q_A| \quad (D.6)$$

where

$$B = a/gA \quad (D.7)$$

$$R = \frac{f\Delta x}{2gDA^2} \quad (D.8)$$

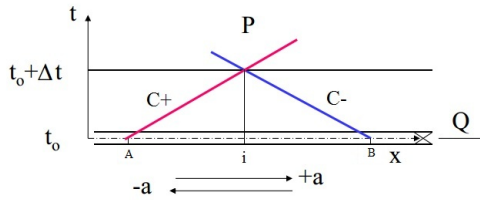


Figure D.1: Usage of C-characteristics in the t-x plane

D.2 Grid representation and computational aspects

The equations needed to compute the head and volumetric flow for each length of pipe in the transient plane have now been derived. For computational purposes, the equations are rewritten in the following notation. (D.5) and (D.6) become

$$H_{p,i} = C_p - BQ_{p,i} \quad (\text{D.9})$$

$$H_{p,i} = C_m + BQ_{p,i} \quad (\text{D.10})$$

$$C_p = H_{i-1} + Q_{i-1} * (B - R|Q_{i-1}|) \quad (\text{D.11})$$

$$C_m = H_{i+1} + Q_{i+1} * (B - R|Q_{i+1}|) \quad (\text{D.12})$$

Combining the above yields

$$H_{p,i} = \frac{1}{2}(C_p + C_m) \quad (\text{D.13})$$

$$Q_{p,i} = \frac{1}{B}(C_p - H_{p,i}) \quad (\text{D.14})$$

The i subscript indicates the coordinate of the section that is currently being analysed, hence, the $i-1$ and $i+1$ are the sections before and after, respectively.

The only unknowns are the H_p and Q_p variables, that represent head and flow for current time increment in the i -position.

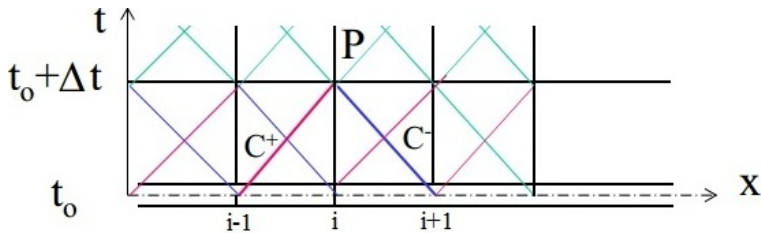


Figure D.2: Collocated position-time grid where pressure and flow are computed in the same points.

(D.13) and (D.14) are suitable for computing flow Q and piezometric head H for all N interior point of the conduit with length L , given that the following conditions are met;

$$dx = \frac{L}{N} \quad (\text{D.15})$$

$$dt = \frac{dx}{a} \quad (\text{D.16})$$

However, for the boundaries of the conduit, we are missing one of the C characteristics. In addition, for the first iteration we require an initial condition to start the simulation.

D.3 Boundary and initial conditions

Initial conditions need to be set before the main iteration can begin. Usually this is a steady state condition of the system that is known before the events that we want to simulate are introduced. For a fluid conduit, this is usually a constant flow combined with standard ideal equation for head loss in a pipe.

$$Q_i = Q_0 = \text{Constant} \quad (\text{D.17})$$

$$H_i = H_0 - (i - 1)RQ_0^2 \quad (\text{D.18})$$

where R is given by (D.8). Note that special initial conditions may exist for each component linked together by the conduit. Flow conditions will change if the system branches, and the linear head computations change with pipe conditions.

As for the boundary conditions, they depend completely on the type of interfacing component. Common for all boundary conditions is that they need one specific equation, containing either Q_p or H_p , that can be combined with either the $C+$ or $C-$ characteristic.

Appendix E

Driva system data

Anleggsbeskrivelse

Driva kraftverk ligger i Sunndal kommune i Møre og Romsdal fylke. I kraftverket utnyttes fallhøyden mellom Gjevilvatn (HRV 660.80 m) og utløpet til elva Driva gjennom to vertikale Francis-aggregater.

Vannvei: Vannveien består av en ca. 19945 m lang tilløpstunnel fra inntaket i Gjevilvatn frem til en finvaregrind oppstrøms ventilkammeret. Til tilløpstunnelen føres fire bekkeinntak, samt avløpet fra Vassli pumpestasjon.

Fram til høybrekket i tunnelen, dvs. for en lengde på ca. 14385 m, har tunnelen et nominelt strømningsstverrsnitt på 20 m². Fra høybrekket og frem til finvaregrinden er tverrsnittet 22 m². Fra inntakskonusen fortsetter vannveien i en stålforet trykksjakt med total lengde på ca. 270 m. Det meste av trykksjakten har diameter 2.30 m, bortsett fra en lengde på ca. 25 m like oppstrøms forgreningen til de to turbinene hvor diameteren går over til 2.10 m.

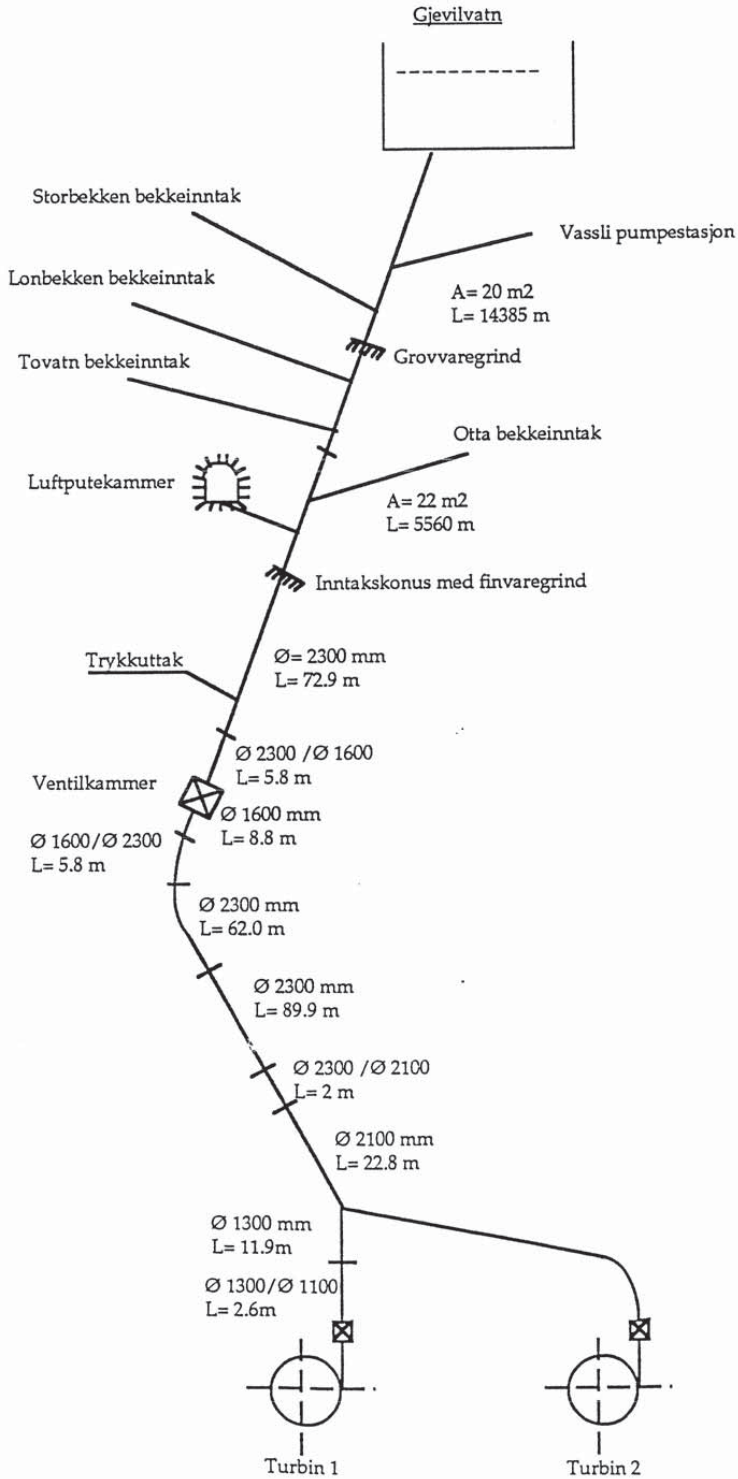
Grennrørene har diameter 1.30 m med overgang til 1.10 m like oppstrøms innløpsventilene. Lengden for grennrør til turbin 1 og turbin 2 er henholdsvis ca. 12 m og ca. 23 m.

Fra utløpet av sugerørene føres vannet i en felles avløpstunnel ut i elva Driva. Avløpstunnelen er ca. 540 m lang med nominelt strømningsstverrsnitt på 22 m².

Vannveien fremgår også av vedlagte skisser.

Turbin 2:	Fabrikat:	Kværner Brug AS / Rainpower (nytt løpehjul)
	År.:	1971 / 2011 (nytt løpehjul)
	Type:	Vertikal Francisturbin
	Fabrikasjons nr.:	3401
	Nom. turbineffekt:	97 000 hk / 82.5 MW (nytt løpehjul)
	Nom. fallhøyde:	540 m
Nom. turtall:	600 o/min.	

Generator 2:	Fabrikat:	Nebb
	Type:	Synkrongenerator WV-295/220/10
	Fabrikasjons nr.:	61384
	Nom. data:	80.000 kVA, cos Ø = 0.9 11000 V 4620 A
	Magnetisering:	180 V / 1130 A



DØRREMSELV:

HRV kt 681,50
LRV kt 677,00
FELT 31,0 km²
GRAVITASJONS-DAM M / VASS-VERK INNTAK:
TAPPELUKE
800 x 1000 mm
LUKE

INNTAKSLUKE:
RULLELUKE
3500 x 4000 mm
MAKS VANN-TRYKK 22,63 m
TERSKEL kt 638,17

GJEVLIVATN:
HRV kt 660,80
LRV kt 645,80
FELT 168,0 km²
MAGASIN 280 M m³

VASSLI PUMPE-STASJON:
SVINGESIAKT:
L = 130 m
F = 4 m²

ÅNGÅRDSVATN / DALSVATN:
HRV kt 582,75
LRV kt 581,25
FELT 81,7 km²
LØSMASSETERSKEL MED 3" SPUNNT

RØRGATE:
L = 178 m
D = 1500 / 2800 mm
MAKS VANN-TRYKK 89,5 m

SPIELDVENTIL:
D = 1500 mm

OTTA:
HRV kt 706,75
LRV kt 704,75
FELT = 35,0 km²

VAKUUMLUKE:
2000 x 1000 mm
MAKS VANNTRYKK 7,75 m
TERSKEL kt 699,0

STORBEKKEN:
HRV kt 677,30
LRV kt 676,80
FELT 5,6 km²
BJELKESTENGSEL

STORLI:
TVERRSLAGSPORT
3000 x 3000 mm
MAKS VANNTRYKK ca. 36,3 m
TERSKEL ca. kt 624,62

SIKTTUNNEL:
L = 110 m / 60 m
F = 4 m² / 13 m²

SIKTTUNNEL:
L = 150 m
F = 12 m²

SIKTTUNNEL:
L = 20 m
F = 4 m²

SIKTTUNNEL:
L = 20 m
F = 4 m²

SIKTTUNNEL:
L = 20 m
F = 4 m²

LONBEKKEN:
HRV kt 683,50
LRV kt 683,00
FELT 15,1 km²
BJELKESTENGSEL

SIKTTUNNEL:
L = 110 m / 60 m
F = 4 m² / 13 m²

SIKTTUNNEL:
L = 150 m
F = 12 m²

SIKTTUNNEL:
L = 20 m
F = 4 m²

SIKTTUNNEL:
L = 20 m
F = 4 m²

SIKTTUNNEL:
L = 20 m
F = 4 m²

FALLBEKKVATNA:
HRV kt 918,90
LRV kt 918,90
FELT 3,8 km²
BJELKESTENGSEL

SIKTTUNNEL:
L = 166 m / 70 m
F = 4 m² / 4 m²

SIKTTUNNEL:
L = 3613 m
F = 6,0 m²

SIKTTUNNEL:
L = 300,0 m
F = 1,3 m²

SIKTTUNNEL:
L = 195 m / 13 m²

SIKTTUNNEL:
L = 150 m
F = 12 m²

SIKTTUNNEL:
L = 150 m
F = 12 m²

TOVATNA:
HRV kt 757,00
LRV kt 756,50
FELT 34,8 km²
MAGASIN 4,5 M m³

SIKTTUNNEL:
L = 100 m
F = 13 m²

SIKTTUNNEL:
L = 100 m
F = 13 m²

SIKTTUNNEL:
L = 100 m
F = 13 m²

SIKTTUNNEL:
L = 100 m
F = 13 m²

SIKTTUNNEL:
L = 100 m
F = 13 m²

FALLBEKKVATNA:
HRV kt 918,90
LRV kt 918,90
FELT 3,8 km²
BJELKESTENGSEL

SIKTTUNNEL:
L = 166 m / 70 m
F = 4 m² / 4 m²

SIKTTUNNEL:
L = 3613 m
F = 6,0 m²

SIKTTUNNEL:
L = 300,0 m
F = 1,3 m²

SIKTTUNNEL:
L = 195 m / 13 m²

SIKTTUNNEL:
L = 150 m
F = 12 m²

SIKTTUNNEL:
L = 150 m
F = 12 m²

FALLBEKKVATNA:
HRV kt 918,90
LRV kt 918,90
FELT 3,8 km²
BJELKESTENGSEL

SIKTTUNNEL:
L = 166 m / 70 m
F = 4 m² / 4 m²

SIKTTUNNEL:
L = 3613 m
F = 6,0 m²

SIKTTUNNEL:
L = 300,0 m
F = 1,3 m²

SIKTTUNNEL:
L = 195 m / 13 m²

SIKTTUNNEL:
L = 150 m
F = 12 m²

SIKTTUNNEL:
L = 150 m
F = 12 m²

FALLBEKKVATNA:
HRV kt 918,90
LRV kt 918,90
FELT 3,8 km²
BJELKESTENGSEL

SIKTTUNNEL:
L = 166 m / 70 m
F = 4 m² / 4 m²

SIKTTUNNEL:
L = 3613 m
F = 6,0 m²

SIKTTUNNEL:
L = 300,0 m
F = 1,3 m²

SIKTTUNNEL:
L = 195 m / 13 m²

SIKTTUNNEL:
L = 150 m
F = 12 m²

SIKTTUNNEL:
L = 150 m
F = 12 m²

FALLBEKKVATNA:
HRV kt 918,90
LRV kt 918,90
FELT 3,8 km²
BJELKESTENGSEL

SIKTTUNNEL:
L = 166 m / 70 m
F = 4 m² / 4 m²

SIKTTUNNEL:
L = 3613 m
F = 6,0 m²

SIKTTUNNEL:
L = 300,0 m
F = 1,3 m²

SIKTTUNNEL:
L = 195 m / 13 m²

SIKTTUNNEL:
L = 150 m
F = 12 m²

SIKTTUNNEL:
L = 150 m
F = 12 m²

FALLBEKKVATNA:
HRV kt 918,90
LRV kt 918,90
FELT 3,8 km²
BJELKESTENGSEL

SIKTTUNNEL:
L = 166 m / 70 m
F = 4 m² / 4 m²

SIKTTUNNEL:
L = 3613 m
F = 6,0 m²

SIKTTUNNEL:
L = 300,0 m
F = 1,3 m²

SIKTTUNNEL:
L = 195 m / 13 m²

SIKTTUNNEL:
L = 150 m
F = 12 m²

SIKTTUNNEL:
L = 150 m
F = 12 m²

FALLBEKKVATNA:
HRV kt 918,90
LRV kt 918,90
FELT 3,8 km²
BJELKESTENGSEL

SIKTTUNNEL:
L = 166 m / 70 m
F = 4 m² / 4 m²

SIKTTUNNEL:
L = 3613 m
F = 6,0 m²

SIKTTUNNEL:
L = 300,0 m
F = 1,3 m²

SIKTTUNNEL:
L = 195 m / 13 m²

SIKTTUNNEL:
L = 150 m
F = 12 m²

SIKTTUNNEL:
L = 150 m
F = 12 m²

FALLBEKKVATNA:
HRV kt 918,90
LRV kt 918,90
FELT 3,8 km²
BJELKESTENGSEL

SIKTTUNNEL:
L = 166 m / 70 m
F = 4 m² / 4 m²

SIKTTUNNEL:
L = 3613 m
F = 6,0 m²

SIKTTUNNEL:
L = 300,0 m
F = 1,3 m²

SIKTTUNNEL:
L = 195 m / 13 m²

SIKTTUNNEL:
L = 150 m
F = 12 m²

SIKTTUNNEL:
L = 150 m
F = 12 m²

FALLBEKKVATNA:
HRV kt 918,90
LRV kt 918,90
FELT 3,8 km²
BJELKESTENGSEL

SIKTTUNNEL:
L = 166 m / 70 m
F = 4 m² / 4 m²

SIKTTUNNEL:
L = 3613 m
F = 6,0 m²

SIKTTUNNEL:
L = 300,0 m
F = 1,3 m²

SIKTTUNNEL:
L = 195 m / 13 m²

SIKTTUNNEL:
L = 150 m
F = 12 m²

SIKTTUNNEL:
L = 150 m
F = 12 m²

FALLBEKKVATNA:
HRV kt 918,90
LRV kt 918,90
FELT 3,8 km²
BJELKESTENGSEL

SIKTTUNNEL:
L = 166 m / 70 m
F = 4 m² / 4 m²

SIKTTUNNEL:
L = 3613 m
F = 6,0 m²

SIKTTUNNEL:
L = 300,0 m
F = 1,3 m²

SIKTTUNNEL:
L = 195 m / 13 m²

SIKTTUNNEL:
L = 150 m
F = 12 m²

SIKTTUNNEL:
L = 150 m
F = 12 m²

FALLBEKKVATNA:
HRV kt 918,90
LRV kt 918,90
FELT 3,8 km²
BJELKESTENGSEL

SIKTTUNNEL:
L = 166 m / 70 m
F = 4 m² / 4 m²

SIKTTUNNEL:
L = 3613 m
F = 6,0 m²

SIKTTUNNEL:
L = 300,0 m
F = 1,3 m²

SIKTTUNNEL:
L = 195 m / 13 m²

SIKTTUNNEL:
L = 150 m
F = 12 m²

SIKTTUNNEL:
L = 150 m
F = 12 m²

FALLBEKKVATNA:
HRV kt 918,90
LRV kt 918,90
FELT 3,8 km²
BJELKESTENGSEL

SIKTTUNNEL:
L = 166 m / 70 m
F = 4 m² / 4 m²

SIKTTUNNEL:
L = 3613 m
F = 6,0 m²

SIKTTUNNEL:
L = 300,0 m
F = 1,3 m²

SIKTTUNNEL:
L = 195 m / 13 m²

SIKTTUNNEL:
L = 150 m
F = 12 m²

SIKTTUNNEL:
L = 150 m
F = 12 m²

FALLBEKKVATNA:
HRV kt 918,90
LRV kt 918,90
FELT 3,8 km²
BJELKESTENGSEL

SIKTTUNNEL:
L = 166 m / 70 m
F = 4 m² / 4 m²

SIKTTUNNEL:
L = 3613 m
F = 6,0 m²

SIKTTUNNEL:
L = 300,0 m
F = 1,3 m²

SIKTTUNNEL:
L = 195 m / 13 m²

SIKTTUNNEL:
L = 150 m
F = 12 m²

SIKTTUNNEL:
L = 150 m
F = 12 m²

FALLBEKKVATNA:
HRV kt 918,90
LRV kt 918,90
FELT 3,8 km²
BJELKESTENGSEL

SIKTTUNNEL:
L = 166 m / 70 m
F = 4 m² / 4 m²

SIKTTUNNEL:
L = 3613 m
F = 6,0 m²

SIKTTUNNEL:
L = 300,0 m
F = 1,3 m²

SIKTTUNNEL:
L = 195 m / 13 m²

SIKTTUNNEL:
L = 150 m
F = 12 m²

SIKTTUNNEL:
L = 150 m
F = 12 m²

FALLBEKKVATNA:
HRV kt 918,90
LRV kt 918,90
FELT 3,8 km²
BJELKESTENGSEL

SIKTTUNNEL:
L = 166 m / 70 m
F = 4 m² / 4 m²

SIKTTUNNEL:
L = 3613 m
F = 6,0 m²

SIKTTUNNEL:
L = 300,0 m
F = 1,3 m²

SIKTTUNNEL:
L = 195 m / 13 m²

SIKTTUNNEL:
L = 150 m
F = 12 m²

SIKTTUNNEL:
L = 150 m
F = 12 m²

FALLBEKKVATNA:
HRV kt 918,90
LRV kt 918,90
FELT 3,8 km²
BJELKESTENGSEL

SIKTTUNNEL:
L = 166 m / 70 m
F = 4 m² / 4 m²

SIKTTUNNEL:
L = 3613 m
F = 6,0 m²

SIKTTUNNEL:
L = 300,0 m
F = 1,3 m²

SIKTTUNNEL:
L = 195 m / 13 m²

SIKTTUNNEL:
L = 150 m
F = 12 m²

SIKTTUNNEL:
L = 150 m
F = 12 m²

FALLBEKKVATNA:
HRV kt 918,90
LRV kt 918,90
FELT 3,8 km²
BJELKESTENGSEL

SIKTTUNNEL:
L = 166 m / 70 m
F = 4 m² / 4 m²

SIKTTUNNEL:
L = 3613 m
F = 6,0 m²

SIKTTUNNEL:
L = 300,0 m
F = 1,3 m²

SIKTTUNNEL:
L = 195 m / 13 m²

SIKTTUNNEL:
L = 150 m
F = 12 m²

SIKTTUNNEL:
L = 150 m
F = 12 m²

FALLBEKKVATNA:
HRV kt 918,90
LRV kt 918,90
FELT 3,8 km²
BJELKESTENGSEL

SIKTTUNNEL:
L = 166 m / 70 m
F = 4 m² / 4 m²

SIKTTUNNEL:
L = 3613 m
F = 6,0 m²

SIKTTUNNEL:
L = 300,0 m
F = 1,3 m²

SIKTTUNNEL:
L = 195 m / 13 m²

SIKTTUNNEL:
L = 150 m
F = 12 m²

SIKTTUNNEL:
L = 150 m
F = 12 m²

FALLBEKKVATNA:
HRV kt 918,90
LRV kt 918,90
FELT 3,8 km²
BJELKESTENGSEL

SIKTTUNNEL:
L = 166 m / 70 m
F = 4 m² / 4 m²

SIKTTUNNEL:
L = 3613 m
F = 6,0 m²

SIKTTUNNEL:
L = 300,0 m
F = 1,3 m²

Appendix F

Rejection Trials Driva

Oppdrag: Avslagsprøver og servovindikering etter bytte av løpehjul
 Måledato: 13. og 14. januar 2010
 Forrige måling: -
 Måling utført av: Leif Parr
 Kontakt hos kunde: Kjetil Stene

SAMMENDRAG OG KONKLUSJON:

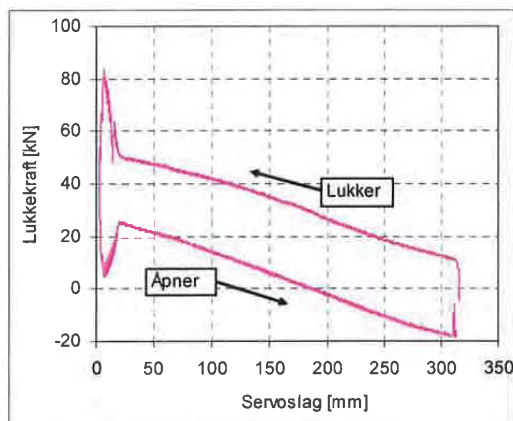
Det ble utført avslags- og servovindikeringsprøver. Resultatene fra avslagsprøvene er oppsummert i tabellen under.

Last før avslag	Ruse- turtall	Max trykk	Trykk før avslag	Rel. ruse- turtall	Aksielt løft aggre- gat	Lukke- tid servo	Tid til full åpning sikker- hets- ventil	Total tid åpen sikker- hets- ventil	Max slag- åpning sikker- hets- ventil
[MW]	[o/min]	[mVs]	[mVs]	[%]	[um]	[s]	[s]	[s]	[mm]
77.9	811	573	524	135.2	-590	8.4	7.1	25.8	100
60.0	764	571	536	127.3	-377	7.7	6.3	20.5	72
44.0	712	572	546	118.6	-200	7.0	5.1	14.5	42
30.0	672	-	-	112.0	-150	-	3.9	10.8	27
15.0	620	-	-	103.3	-65	-	2.2	6.4	11

Forbislipningsventilen åpner ved alle avslag. Trykket stiger lite under avslag, og har god margin på tillatt stigning. Turtallet stiger som forventet, og overstiger så vidt tillatt turtallstigning ved avslag fra 78MW (135.2% turtallsstigning).

Vi anbefaler at avslagsprøvene godkjennes.

Resultater fra servovindikeringen er vist i figuren til høyre. Regulatoren har tilfredsstillende kraftreserver i forhold til kreftene i ledeapparatet.



Oppdragsgiver

Trønderenergi

Sak

DRIVA

Aggregat 1

Avslagsprøver og servovindikering

Rapport

Utarbeidet

Leif Parr

Fagkontrollert

Andre Reynaud

Godkjent

Eivind Oppedal Olsen

Dato

1. februar 2010

Norconsult

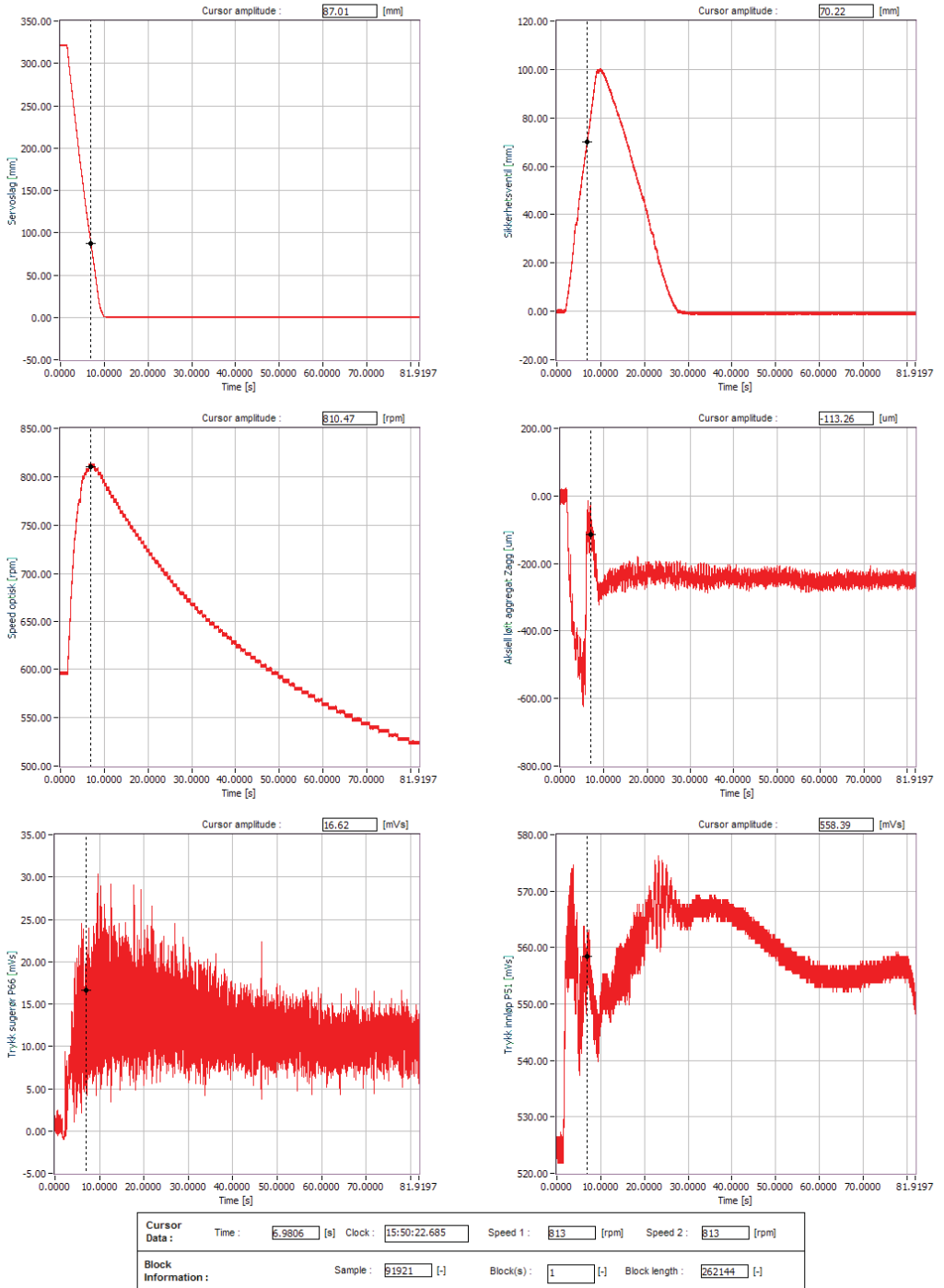
Dokumentnr.

lpa_Driva1_avslagv01.doc

Revisjon

0

Company : TronderEnergi
 Plant/Unit : Driva Agg 1
 File Path : C:\data\20100113_avslag\avslag78MW_1549.dat



Figur 9 Avslag fra 78 MW

Sammendrag

Oppdrag: Avslagsprøver, servoindikering og vibrasjonsmåling ved idriftsettelse av Aggregat 2, etter skifte av løpehjul (vibrasjonsmåling rapporteres i separat rapport)

Måledato: 4. jan 2012

Forrige måling: 29. mars 1999

Måling utført av: Einar Kobro

Kontakt hos kunde: Kjetil Stene

Det ble utført servoindikering og avslagsprøver. Hovedresultatene for avslagene er gitt i tabellen under:

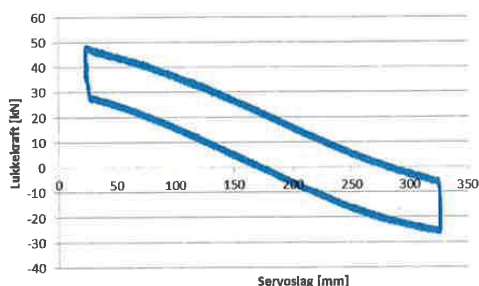
Last før avslag	Max turtall	Max turtall rel	Maks trykk	Rel. trykkstigning	Aksielt løft øv kryss. *)	Lukketid servo
MW	rpm	%	mvs	%	um	s
20	630	105	590	104	-40	2.1
40	685	114	592	105	-100	3.4
60	743	124	598	105	-130	4.5
81	817	136	601	106	-229	5.9

*) negativt løft indikerer nedbøy av øvre kryss

Turtalls- og trykkstigning (817 rpm og 601 mvs) ligger under verdiene antydnet i tilbudet (840 rpm og 681 mvs). Servoens lukketid ved fullastavslag (6 sek) ligger under verdien antydnet i tilbudet (8 sek).

Vi anbefaler at avslagsprøvene godkjennes.

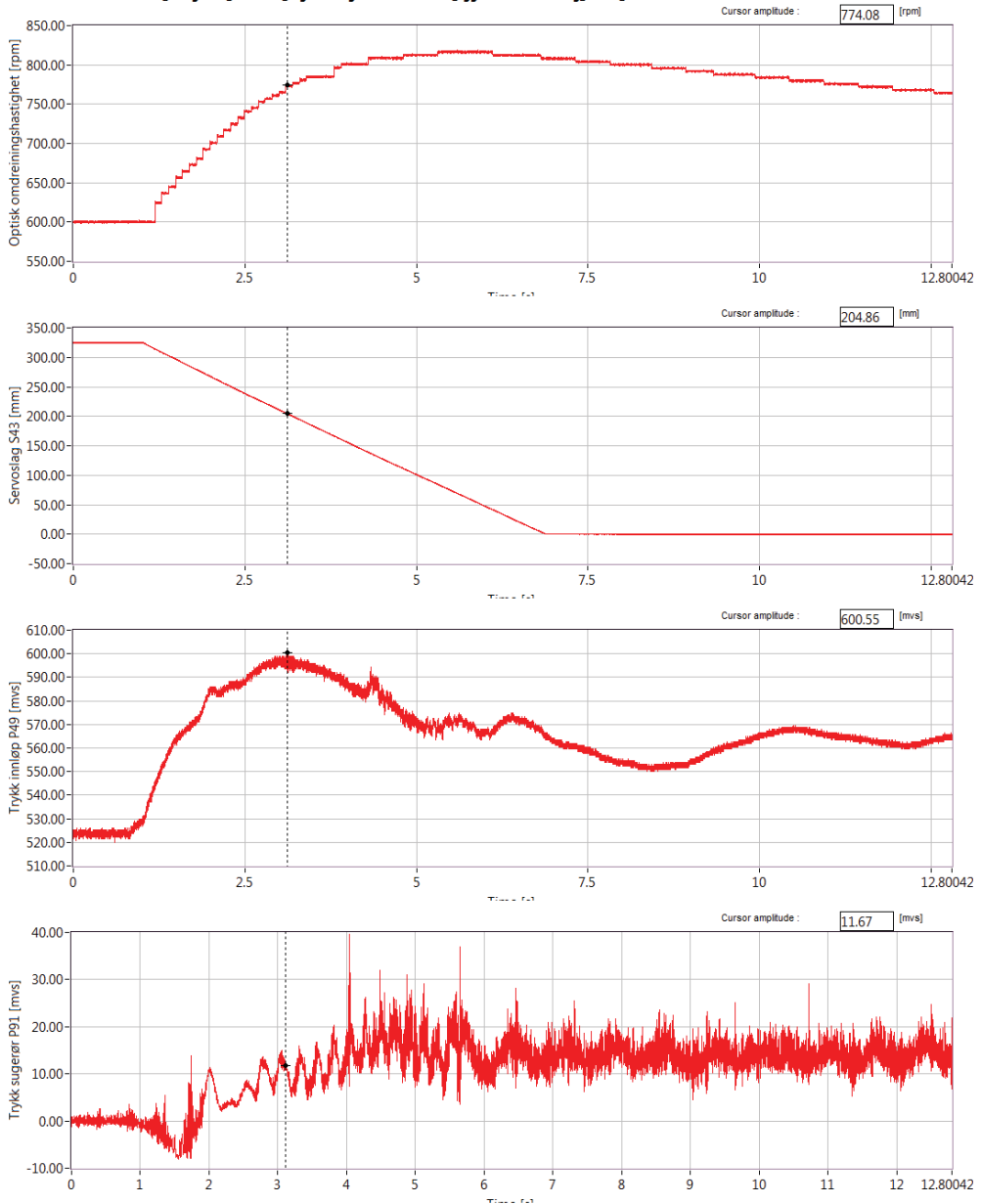
Resultatene fra servoindikeringen vises i figuren til høyre. Regulatoren har tilstrekkelige kraftreserver.



01	2012-01-18	Rapport	Einar Kobro	Leif Parr	Eivind Oppedal Olsen
Rev.	Dato:	Beskrivelse	Utarbeidet	Fagkontroll	Godkjent

Dette dokumentet er utarbeidet av Norconsult AS som del av det oppdraget som dokumentet omhandler. Opphavsretten tilhører Norconsult. Dokumentet må bare benyttes til det formål som oppdragsavtalen beskriver, og må ikke kopieres eller gjøres tilgjengelig på annen måte eller i større utstrekning enn formålet tilsier.

Company : TronderEnergi
Plant/Unit : Driva Agg 2
File Path : J:\50_Energi\540_Maskin\3_Fag:Erfaring\Data\2012\Driva_agg2\20120104\avslag_81MW_1555.dat



Cursor Data:	Time : 3.1131 [s]	Clock : 15:56:05.6799	Speed 1 : 782 [rpm]	Speed 2 : NaN [rpm]
Block Information:	Sample : 17236 [t]	Block(s) : 2 [t]	Block length : 32768 [t]	

Figur A.3-6 Avslag fra 81MW